

AD 745214

AD

# USAAMRDL TECHNICAL REPORT 72-22

## INVESTIGATION OF THE SPEED BRAKES ON THE S-67 AIRCRAFT

By

N. F. K. Kefford

May 1972

**EUSTIS DIRECTORATE  
U. S. ARMY AIR MOBILITY RESEARCH AND DEVELOPMENT LABORATORY  
FORT EUSTIS, VIRGINIA**

CONTRACT DAAJ02-71-C-0009  
UNITED AIRCRAFT CORPORATION  
SIKORSKY AIRCRAFT DIVISION  
STRATFORD, CONNECTICUT

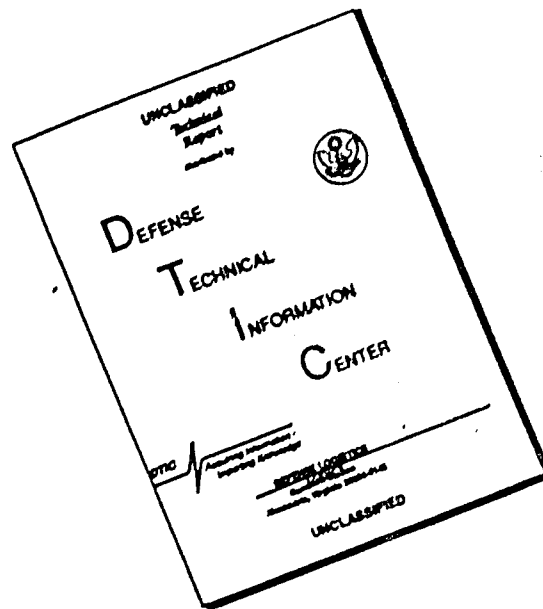
D D C  
RECEIVED  
JUL 17 1972  
C

Approved for public release;  
distribution unlimited.



Reproduced by  
NATIONAL TECHNICAL  
INFORMATION SERVICE  
U S Department of Commerce  
Springfield VA 22151

# DISCLAIMER NOTICE



THIS DOCUMENT IS BEST QUALITY AVAILABLE. THE COPY FURNISHED TO DTIC CONTAINED A SIGNIFICANT NUMBER OF PAGES WHICH DO NOT REPRODUCE LEGIBLY.

#### DISCLAIMERS

The findings in this report are not to be construed as an official Department of the Army position unless so designated by other authorized documents.

When Government drawings, specifications, or other data are used for any purpose other than in connection with a definitely related Government procurement operation, the United States Government thereby incurs no responsibility nor any obligation whatsoever; and the fact that the Government may have formulated, furnished, or in any way supplied the said drawings, specifications, or other data is not to be regarded by implication or otherwise as in any manner licensing the holder or any other person or corporation, or conveying any rights or permission, to manufacture, use, or sell any patented invention that may in any way be related thereto.

Trade names cited in this report do not constitute an official endorsement or approval of the use of such commercial hardware or software.

#### DISPOSITION INSTRUCTIONS

Destroy this report when no longer needed. Do not return it to the originator.

ACCESSION for	
CFSTI	WHITE SECTION <input checked="" type="checkbox"/>
DDC	DIFF SECTION <input type="checkbox"/>
UNANNOUNCED	<input type="checkbox"/>
JUSTIFICATION	
BY	
DISTRIBUTION/AVAILABILITY CODES	
DIST.	AVAIL. and/or SPECIAL
A	

Unclassified  
Security Classification

DOCUMENT CONTROL DATA - R & D		
(Security classification of title, body of abstract and indexing annotation must be entered when the overall report is classified)		
1. ORIGINATING ACTIVITY (Corporate author) Sikorsky Aircraft Division United Aircraft Corporation Stratford, Connecticut		2a. REPORT SECURITY CLASSIFICATION Unclassified 2b. GROUP
3. REPORT TITLE INVESTIGATION OF THE SPEED BRAKES ON THE S-67 AIRCRAFT		
4. DESCRIPTIVE NOTES (Type of report and inclusive dates) Final Report		
5. AUTHOR(S) (First name, middle initial, last name) N.F.K. Kefford		
6. REPORT DATE April 1972	7a. TOTAL NO. OF PAGES 57	7b. NO. OF REFS 4
8a. CONTRACT OR GRANT NO. DAAJ02-71-C-0009 b. PROJECT NO.	9a. ORIGINATOR'S REPORT NUMBER(S) USAAMRDL Technical Report 72-22	
c. Task 1F163204D15704 d.	9b. OTHER REPORT NO(S) (Any other numbers that may be assigned this report) SER-67007	
10. DISTRIBUTION STATEMENT Approved for public release; distribution unlimited.		
11. SUPPLEMENTARY NOTES	12. SPONSORING MILITARY ACTIVITY Eustis Directorate U.S. Army Air Mobility R&D Laboratory Fort Eustis, Virginia	
13. ABSTRACT Under Contract DAAJ02-71-C-0009, Sikorsky Aircraft conducted flight tests and computer simulations to evaluate speed brakes for a winged helicopter.  The flight test program established the effectiveness of wing-mounted speed brakes for increasing dive angle, deceleration capability, and maneuverability of the Sikorsky S-67. In the configuration tested, six brake surfaces operated together to increase aircraft drag by 155% while reducing wing lift. With these speed brakes, dive angles could be increased from 5 to 7 degrees at 140 knots dependent upon the initial dive angle. At 160 knots, the increase in dive angle varies from 8 to 9 degrees. These increases in aircraft dive angle due to speed brake extension can be further increased by allowing the aircraft to accelerate during the dive.  Dive characteristics with and without speed brakes extended were obtained. A dive envelope defined by control and airframe stress limits was established that provided a broad dive envelope of forward speed and collective settings to achieve various dive angles.  Above dive speeds of 120 knots, the brakes caused a decrease in fuselage attitude to the flight path of 4 to 5 degrees, for a given dive angle. This, coupled with the steeper dive angles, improves the aircraft's capability as a weapons platform.  Speed brakes enabled constant-altitude deceleration from 180 to 140 knots in 9 seconds as compared to 24 seconds with a clean wing.  The computer simulation program examined increased brake area, variable stabilator bias angle, and the consequences of asymmetric brake deployment. Steady dive angles of 30 degrees or more were possible with increased brake area. Following any configuration of asymmetric brake deployment, there was always sufficient roll control power to restore and hold trim, although some deceleration occurred due to collective and/or power limits.		

DD FORM 1473  
1 NOV 65

REPLACES DD FORM 1473, 1 JAN 64, WHICH IS  
OBSOLETE FOR ARMY USE.

Unclassified  
Security Classification

Unclassified

Security Classification

14	KEY WORDS	LINK A		LINK B		LINK C	
		ROLE	WT	ROLE	WT	ROLE	WT
	Helicopter Winged Helicopter Sikorsky S-67 Aerodynamics Dive Deceleration Maneuverability Speed Brakes						

Unclassified

Security Classification

11a



DEPARTMENT OF THE ARMY  
U. S. ARMY AIR MOBILITY RESEARCH & DEVELOPMENT LABORATORY  
EUSTIS DIRECTORATE  
FORT EUSTIS, VIRGINIA 23604

This report was prepared by United Aircraft Corporation, Sikorsky Aircraft Division, under Contract DAAJ02-71-C-0009.

The program was a flight investigation of wing-mounted speed brakes as installed on the S-67 winged helicopter. A computer simulation study was included to determine the effects of increased brake area, variable stabilator bias angle, and asymmetric brake deployment. This program is one of four flight investigations conducted on the S-67 winged helicopter. The other three flight investigations were concerned with a stabilator, a force-feel control system, and aircraft maneuverability.

The wing-mounted speed brakes on the S-67 aircraft increase the dive angle and reduce the fuselage attitude relative to the flight path. At 140 knots airspeed, the increase in dive angle varies from 5 to 7 degrees dependent upon the initial dive angle. At 160 knots, the increase in dive angle varies from 8 to 9 degrees. The aircraft dive angle may be further increased by allowing the aircraft to accelerate during the dive. The amount of reduction in fuselage angle relative to the flight path varies from 4 to 5 degrees for all airspeeds above 120 knots. The speed brakes enable the S-67 aircraft to be decelerated in level flight from 180 to 140 knots in 9 seconds as compared to 24 seconds without the use of brakes.

The report has been reviewed by this Directorate and is technically correct.

This program was conducted under the technical management of Mr. R. C. Dumond of the Applied Aeronautics Division.

Task 1F163204D15704  
Contract DAAJ02-71-C-0009  
USAAMRDL Technical Report 72-22  
May 1972

INVESTIGATION OF THE SPEED BRAKES ON  
THE S-67 AIRCRAFT

SER-67007

by

N. F. K. Kefford

Prepared by

United Aircraft Corporation  
Sikorsky Aircraft Division  
Stratford, Connecticut

for

EUSTIS DIRECTORATE  
U. S. ARMY AIR MOBILITY RESEARCH AND DEVELOPMENT LABORATORY  
FORT EUSTIS, VIRGINIA

Approved for public release; distribution unlimited.
---

ii c.

### ABSTRACT

Under Contract DAAJ02-71-C-0009, Sikorsky Aircraft conducted flight tests and computer simulations to evaluate speed brakes for a winged helicopter.

The flight test program established the effectiveness of wing-mounted speed brakes for increasing dive angle, deceleration capability, and maneuverability of the Sikorsky S-67. In the configuration tested, six brake surfaces operated together to increase aircraft drag by 155% while reducing wing lift. With these speed brakes, dive angles could be increased from 5 to 7 degrees at 140 knots dependent upon the initial dive angle. At 160 knots, the increase in dive angle varies from 8 to 9 degrees. These increases in aircraft dive angle due to speed brake extension can be further increased by allowing the aircraft to accelerate during the dive.

Dive characteristics with and without speed brakes extended were obtained. A dive envelope defined by control and airframe stress limits was established that provided a broad dive envelope of forward speed and collective settings to achieve various dive angles.

Above dive speeds of 120 knots, the brakes caused a decrease in fuselage attitude to the flight path of 4 to 5 degrees, for a given dive angle. This, coupled with the steeper dive angles, improves the aircraft's capability as a weapons platform.

Speed brakes enabled constant-altitude deceleration from 180 to 140 knots in 9 seconds as compared to 24 seconds with a clean wing.

The computer simulation program examined increased brake area, variable stabilator bias angle, and the consequences of asymmetric brake deployment. Steady dive angles of 30 degrees or more were possible with increased brake area. Following any configuration of asymmetric brake deployment, there was always sufficient roll control power to restore and hold trim, although some deceleration occurred due to collective and/or power limits.



## FOREWORD

This report presents results of flight tests and computer simulations to investigate the effectiveness of speed brakes for increasing dive angle, deceleration capability, and maneuverability of the S-67 aircraft. This program is part of a four-phase investigation of the flight characteristics of the S-67 aircraft as a representative high-speed winged helicopter. Investigations of the stabilator, aircraft maneuverability, and a Feel Augmentation System (FAS) are also part of the flight investigation of the S-67. The FAS is a system to provide "force-feel" in pitch.

The work was performed by the Sikorsky Aircraft Division of United Aircraft Corporation for the U.S. Army Air Mobility Research and Development Laboratory, Fort Eustis, Virginia, under Contract DAA-102-71-C-0009, LA Task 1F163204D15704. Mr. E. C. Dumond was the Army technical representative.

**Preceding page blank**

# TABLE OF CONTENTS

ABSTRACT . . . . .	Page iii
FOREWORD . . . . .	v
LIST OF ILLUSTRATIONS . . . . .	viii
LIST OF SYMBOLS . . . . .	x
INTRODUCTION . . . . .	1
DESCRIPTION OF AIRCRAFT . . . . .	2
THE S-67 SPEED BRAKES . . . . .	6
FLIGHT TEST CONDITIONS . . . . .	7
Loading . . . . .	7
Flight . . . . .	7
Stabilator Bias Angle . . . . .	7
RESULTS AND DISCUSSION . . . . .	8
Level Flight . . . . .	8
Dive Angle and Fuselage Angle of Attack . . . . .	8
Dive Envelope . . . . .	9
Maximum Engine Torque Limit . . . . .	10
Minimum Engine Torque Limit . . . . .	10
Main Rotor Control Loads . . . . .	10
Stabilator Vibratory Stress . . . . .	10
Lack of Right Pedal Control . . . . .	11
Speed Brake Extension and Retraction, Controls Fixed . . . . .	11
Accelerations and Turns . . . . .	11
Computer Simulation Study . . . . .	12
Increased Brake Effectiveness . . . . .	12
Effect of Stabilator Bias Angle . . . . .	12
Asymmetric Deployment . . . . .	13
CONCLUSIONS . . . . .	14
LITERATURE CITED . . . . .	15
APPENDIXES	
I. S-67 Wind Tunnel Data . . . . .	39
II. Computer Simulation Study . . . . .	41
DISTRIBUTION . . . . .	48

# LIST OF ILLUSTRATIONS

<u>Figure</u>		<u>Page</u>
1	The S-67 Aircraft, Quarter View . . . . .	16
2	Speed Brake Areas and Locations . . . . .	17
3	In-Flight Front View, Speed Brakes Retracted . . . . .	18
4	In-Flight Front View, Speed Brakes Extended . . . . .	18
5	Speed Brake Controls . . . . .	19
6	Trim Level-Flight Characteristics, GW = 17,300 lb, cg = 258 in. . . . .	20
7	Trim Level-Flight Characteristics, GW = 14,800 lb, cg = 276 in. . . . .	21
8	Trim Level-Flight Characteristics, GW = 17,300 lb, cg = 276 in. . . . .	22
9	Dive Characteristics, GW = 14,800 lb, cg = 276 in., Speed Brakes Extended . . . . .	23
10	Dive Characteristics, GW = 17,300 lb, cg = 276 in., Speed Brakes Retracted . . . . .	24
11	Dive Characteristics, GW = 17,300 lb, cg = 276 in., Speed Brakes Extended . . . . .	25
12	Fuselage Angle of Attack, GW = 17,300 lb, cg = 276 in., V = 140 kt. . . . .	26
13	Fuselage Angle of Attack vs. Engine Torque and Forward Speed, GW = 17,300 lb, cg = 276 in., Speed Brakes Extended . . . . .	27
14	Simulation of Dive Characteristics, Speed Brakes Retracted, GW = 14,800 lb, cg = 276 in. . . . .	28
15	Simulation of Dive Characteristics, Speed Brakes Extended, GW = 14,800 lb, cg = 276 in. . . . .	29
16	Collective vs. Engine Torque, GW = 17,300 lb, cg = 276 in..	30
17	Dive Angle vs. Engine Torque and Forward Speed, GW = 17,300 lb, cg = 276 in., Speed Brakes Extended . . . . .	31
18	Tail Rotor Pitch vs. Engine Torque and Forward Speed, GW = 17,300 lb, cg = 276 in., Speed Brakes Extended . . . . .	32

<u>Figure</u>		<u>Page</u>
19	Transient Effects of Speed Brake Extension at $V = 180$ kt, Controls Fixed . . . . .	33
20	Deceleration From $V = 180$ to $V = 140$ kt, Without Speed Brakes . . . . .	34
21	Deceleration From $V = 180$ to $V = 140$ kt, With Speed Brakes . . . . .	35
22	Simulation of Dive Characteristics, Speed Brakes Extended, $GW = 14,800$ lb, $cg = 276$ in., Double Existing Brake Area . . . . .	36
23	Simulation of Dive Characteristics, Speed Brakes Extended, $GW = 14,800$ lb, $cg = 276$ in., Stabilator Bias Angle = $5.0$ deg . . . . .	37
24	Speed Brake Panel Identification . . . . .	38
25	S-67 Wind Tunnel Data, Showing Lift, Pitching Moment, and Drag vs. Fuselage Angle of Attack for Total Aircraft Less Wings, With Wings, and Speed Brakes Retracted and Extended . . . . .	40
26	Comparison Between Simulated and Flight Test Data, Level Flight Trim, $GW = 14,800$ lb, $cg = 276$ in., Stabilator Bias = $0$ deg, Speed Brakes Retracted . . . . .	43
27	Comparison Between Simulated and Flight Test Data, Level Flight Trim, $GW = 14,500$ lb, $cg = 275$ in., Stabilator Bias = $0$ deg, Speed Brakes Extended . . . . .	45
28	Comparison Between Simulated and Flight Test Data, Level Flight Trim, $GW = 16,800$ lb, $cg = 258$ in., Stabilator Bias = $2.5$ deg, Speed Brakes Extended . . . . .	46
29	Comparison Between Simulated and Flight Test Data, Level Flight Trim, $GW = 17,200$ lb, $cg = 275$ in., Stabilator Bias = $2.5$ deg, Speed Brakes Extended . . . . .	47

### LIST OF SYMBOLS

$A_{1s}$	lateral cyclic control, %
$B_{1s}$	longitudinal cyclic control, %
$i_t$	stabilator incidence angle, deg
$N_R$	main rotor speed, rpm
$S_E$	required engine torque, %
$RCD$	rate of descent, fpm
$CP$	required shaft horsepower, hp
$V$	forward speed, kt
$V_{max}$	maximum level-flight forward speed, kt
$\alpha$	fuselage angle of attack, deg
$\beta$	fuselage sideslip angle, deg
$\gamma$	dive angle, deg
$\theta_{TR}$	tail rotor blade pitch, deg
$\theta_f$	fuselage pitch attitude, deg
$\theta_0$	main rotor collective control, %
$\theta_{cuff}$	main rotor collective blade pitch, deg
$\phi_f$	fuselage roll attitude, deg

## INTRODUCTION

Experience with high-performance helicopters has indicated that aerodynamic speed brakes would improve control characteristics and maneuverability. They should reduce aircraft acceleration in a dive as well as reduce wing lift. This would permit steeper dives and rapid decelerations.

Wind tunnel testing of the aerodynamic effects of speed brakes resulted in the present arrangement of six unperforated panels mounted on the wings of the S-67 aircraft.

The speed brakes on the S-67 aircraft were evaluated in flight tests to determine their effectiveness for increasing dive angle, deceleration capability and maneuverability on a high-speed winged helicopter. The test results were correlated with a computer simulation study, and the simulation was used to predict the effects of different brake areas, stabilator bias angle and asymmetric brake deployment.

### DESCRIPTION OF AIRCRAFT

The S-67 demonstrator is a high-speed derivative of the Sikorsky SH-3D helicopter. A view of the aircraft is presented in Figure 1. The low-drag airframe was designed to meet requirements of an attack mission. The cockpit is arranged in tandem, with the gunner in the forward seat and the pilot in the aft, elevated seat. The pilot has visibility down to minus 15 degrees over the nose. Two T50-GR-5 engines are mounted in one main rotor pylon above the fuselage center section.

Main rotor hub, tail rotor, drive system, and transmission systems are all SH-3D dynamic components. The main rotor has five S-61F blades, each with a twist of -4 degrees. The 22-inch blade tips are swept back 20 degrees to delay tip Mach number effects. The control system uses SH-3D components and the CH-54 automatic flight control system.

The fixed-wing type control surfaces include a stabilator, a fixed vertical stabilizer, and sponsons with stub wings for additional lift. The tail wheel is attached to the base of the ventral fin, and the retractable main landing gear is housed in the wing. The wing panels have speed brakes to control dive angle and increase deceleration capability. Flight control sensitivities are listed in the table below.

FLIGHT CONTROL SENSITIVITIES				
	Servo Travel per Inch (%)	Blade Pitch per Inch (%)	Stick/Pedal Travel (in.)	Blade Pitch Travel (deg)
Longitudinal Cyclic	7.2	1.7	14	24
Lateral Cyclic	7.2	1.4	14	16
Pedals	24.6*	7.75 (Tail Rotor)	4.07*	31.5 (Tail Rotor)
Collective	10.5	1.7	9.5	16
* Working range, at constant collective				

Principal dimensions and general data for the S-67 aircraft are as follows:

Main Rotor

Diameter	62 ft
Normal Tip Speed (104% $N_R$ )	686 ft/sec
Disc Area	3019 ft <sup>2</sup>
Solidity	0.0781
Number of Blades	5
Blade Chord	1.52 ft
Blade Twist	-4 deg
Airfoil Section	NACA 0012 MOD
Articulation	Full Flapping and Lagging
Tip Sweep	20 deg

Tail Rotor

Diameter	10 ft 4 in.*
Tip Speed	700 ft/sec
Disc Area	83.9 ft <sup>2</sup>
Solidity	0.1885
Number of Blades	5
Blade Chord	0.612 ft
Blade Twist	0 deg
Airfoil Section	NACA 0012 MOD
Pitch Flap Coupling	45 deg

---

\* During flight tests, diameter was increased 3 in. to 10 ft. 7 in. to increase lateral low-speed flight capability.



### Fuselage

Overall Length	64 ft 1 in.
Overall Height	16 ft 3 in.
Overall Width	27 ft 4 in.
Wheel Tread	7 ft
Wheel Base	36 ft 2 in.

### Stabilator

Root Chord	4 ft 2 in.
Tip Chord	2 ft
Taper Ratio	0.48
Area	50 ft <sup>2</sup>
Span	15 ft 6 in.
Aspect Ratio	4.8
Airfoil (Root)	NACA 0015
Airfoil (Tip)	NACA 0012

### Vertical Fin

Root Chord	7 ft 6 in.
Tip Chord (Upper)	2 ft 10 in.
Tip Chord (Lower)	3 ft 9 in.
Taper Ratio (Upper)	0.62
Taper Ratio (Lower)	0.5
Total Area	68.7 ft <sup>2</sup>
Aspect Ratio	2.65
Airfoil Section	NACA 4415

### Wing

Root Chord	4 ft 6 in.
Tip Chord	1 ft 11.5 in.
Overall Span	27 ft 4 in.
Total Exposed Area	58 ft <sup>2</sup>
Incidence	8 deg
Dihedral	10 deg
Quarter Chord Sweep	10 deg 15 min
Taper Ratio (Exposed)	0.44
Aspect Ratio	8.0

Wing (cont'd)

Airfoil Section, Root

NACA 4415

Airfoil Section, Tip

NACA 4411

Propulsion System

Engines

Two T58-GE-6

Takeoff Power (Each)

1500 HP

Military Power

1400 HP

Normal Power

1250 HP

Transmission Rating

2800 HP (111% engine torque)

Loading Conditions

Empty Weight\*

10900 lb

Maximum Gross Weight Flown

18000 lb

Maximum Gross Weight Capability

21800 lb

Center-of-Gravity Range

258 in. to 276 in.

\*Aircraft less fuel, payload, and crew.

### THE S-67 SPEED BRAKES

Initial wind tunnel testing of a one-twelfth scale model of the S-67 evaluated an aerodynamic braking surface attached to the main landing gear (Reference 1). Evaluation of other speed brake locations (fuselage, wing, and ventral fin) indicated that wing-mounted surfaces were the most effective. Wind tunnel data predicted an increase of 155% in total aircraft drag at zero fuselage incidence. Moreover, wing lift could be reduced for better autorotation characteristics, and for roll control through asymmetric deployment.

Figure 2 shows the location and dimensions of the S-67 speed brakes. Figures 3 and 4 show in-flight front views of the aircraft clean and with brakes extended. The unperforated brake panels lie flush with the wing surface under normal flight conditions, and extend to a position at right angles to the wing chordline. All brake surfaces are actuated by a single hydraulic actuator. Normal time for opening or closing brakes is 1.6 seconds. The actuator control is on the pilot's collective stick, and the emergency retraction switch is on the emergency panel (Figure 5).

Wind tunnel data are presented in Appendix 1, showing the effects of the wing and speed brakes on total aircraft lift, pitching moment, and drag, as a function of fuselage attitude,  $\alpha$ , relative to the free stream.

## FLIGHT TEST CONDITIONS

### LOADING

Listed below are the combinations of gross weight and altitudes flown at various locations that were flown. A forward center of gravity, at maximum gross weight, was not flown because it could only fly at altitudes of a very low gross load. However, this loading condition was investigated in the simulation study.

<u>Load Condition</u>	<u>Gross Weight</u>	<u>Altitude</u>
#1	17,100	
#2	17,800	
#3	17,300	

### FLIGHT

In-flight gross weight varied from 17,100 to 17,800 pounds. The altitude of 3,000 feet. For the high descent rate of interest in the basic study, it was necessary to commence partial power descent at a density altitude of 4,000 feet.

### STABILATOR PITCH ANGLE

The stabilator pitch angle of 1.5 degrees leading edge down was selected for level flight with speed brakes retracted. This setting provided an overall minimum level of flapping and main rotor vibration, adequate longitudinal control margin, and a body pitch angle to preserve positive wing lift at high speeds. Therefore, it provides the results of an evaluation of the effects of stabilator pitch angle.

## RESULTS AND DISCUSSION

### LEVEL FLIGHT

Figures 1, 2, and 3 compare  $C_{L, \text{max}}$ ,  $C_{D, \text{max}}$ , and aircraft attitudes with and without speed brakes extended. When the speed brakes are extended, a nose-down pitching moment results. To correct for this, changes in longitudinal cyclic pitch of less than 1% are required. To compensate for the loss in wing lift, collective pitch is increased.

### LIVE ANGLE AND FLAPING ANGLE FLIGHT

At speeds between  $V_{\text{min}}$  and  $V_{\text{max}}$ , lives were made for at least three engine torque settings for each live speed: the torque that would be required for level flight, the minimum torque to maintain 10%  $q_y$ , and an intermediate torque setting. Thus, values of engine torque versus forward speed were obtained at constant live angle or constant flapwise angle of attack. Figures 4a, 4b, and 4c show data for the 10%  $q_y$  lift condition with speed brakes extended, and the 10%  $q_y$  lift condition with and without speed brakes extended. Figures 4a and 4b show schematically the values of  $q_y$ ,  $q_z$ , and  $q_x$  for maximum live angle at a flight speed of 100 mph, 100 mph with speed brakes retracted and extended. Figure 4c shows the relationship between flapwise angle of attack and live angle.

Knowledge and control of the flapwise attitude in flight path,  $q_z$ , is important if the pilot is required to direct a weapon or landing device, fixed to the aircraft, to various points in the ground. The live charts derived from flight test data, Figures 4a, 4b, and 4c, show scatterable variations in  $q_z$ . This angle becomes as high as 10 degrees  $q_z$  for the steepest lives as the rotor approaches a hover attitude. These values of constant  $q_y$  were derived from test data; that is, by using plots from curves of  $q_y$  versus  $q_z$  at constant flight speed, as illustrated in Figure 1d.

It is desirable to limit the variation in  $q_z$  as much as possible and in particular to prevent the tendency to steep lives, even with aft flap deflection, to provide the pilot greater stability over the ground. A comparison of Figures 4a and 4b shows that, for a given live angle and flight speed, flapwise angle of attack is significantly reduced by the speed brakes. Figure 4c shows  $q_z$  versus live angle at a speed of 100 mph with and without speed brakes extended, showing that as the flap is raised to about 10 degrees at any given live angle, with the speed brakes, the flap creates a 10-degree steeper live at the same  $q_z$  and forward speed. The reduction in flapwise angle of attack and the increase in live angle due to the speed brakes improve the aircraft's capability as a weapon platform.

The live charts, Figures 1, 2, 3, and 4, all show that up to almost constant engine power at flight speed, it is possible, therefore, to operate directly in the live angle range.

Because the live charts, Figures 1, 2, 3, and 4, all show that up to almost constant engine power at flight speed, it is possible, therefore, to operate directly in the live angle range. The results were not fully substantiated in flight testing, but were confirmed with and without traces extended at this level which was obtained by means of the simulator program. These results are shown in Figures 10 and 11. The correlation of flight test data with the simulator data is discussed in Appendix II. Difficulty was experienced in the traces-extended case in simultaneous correlation of flight test data with simulated data for engine power, engine torque, and aircraft attitude. For this reason, engine power in Figure 11 is low, as much as 10%.

Engine torque is not a function of live angle for all forward speeds, as shown for the 100-110 mph. at altitude in Figure 10. Figure 11 shows a comparison of live angle flight test data taken with speed traces extended. The plotted speeds in Figures 10, 11, and 12 are average calibrated airspeeds over each group of test data at nominally constant speed.

#### LIVE ANGLE

Flight test results also substantiated a live curve, as defined by stress and engine reliability limits, which are discussed below. Data were not taken above the limit speeds shown in Figures 1, 2, 3, and 4. Figures 10, 11, and 12 show the individual live curves, respectively described by the accompanying live charts, Figures 10, 11, and 12. By comparison of Figures 10 and 11, at a live angle of 10 degrees, a maximum live angle of 10 degrees is possible at a flight speed of 100 mph, with speed traces retracted. With traces extended, Figure 11a, the maximum live angle is 10 degrees, also at 100 mph. From Figures 10 and 11a, at the lighter or as weight but same gross weight, live angles are generally about 1 degree less, at the same speed and engine power, and by 10 to 15 degrees less.

In all cases above, lives are at constant altitude with even steeper lives possible if the aircraft is permitted to accelerate. The limits as they define the curve are identified in the following table, and note is recommended for expanding the chart.

Live angles steeper than the indicated limits are not shown in the chart. The effect of altitude area is indicated in the upper simulation study report. It is probable that a 10-degree live angle is possible at 100 mph with the indicated engine area, even the present traces at 100 mph. The aircraft's performance is not indicated.



### Lack of Right Pedal Control

The C-47 has a cambered vertical tail surface to reduce tail rotor thrust requirements in high-speed level flight. As the aircraft accelerates in a dive and main rotor torque is reduced, more right pedal is required to offset the side force caused by the vertical tail surface. Referring to Figure 10, as engine torque is decreased at constant airspeed, the tail rotor blade pitch angle approaches the negative limit of -7 degrees to maintain trim. Reference 3 specifies a control margin of 10° of travel, so that tail rotor blade angle should not exceed -4 degrees.

This limitation may be eased by extending the tail rotor negative pitch limit, if no undesirable tail rotor instabilities develop at high negative blade pitch. Alternatively, the center of the vertical fin might be reduced. This would lead to greater tail rotor thrust in level flight, with associated penalties in forward speed capability and tail rotor stresses. Increasing tail rotor rpm would eliminate all restrictions to the yaw control system.

### Speed Brake Extension and Retraction, "STIFF" Flight

The aircraft transient responses to speed brake extension with fixed controls were obtained at speeds from 100 to 170 knots. Figure 11 shows time histories for a speed of 120 knots. The extension produces a moment and loss of wing lift as brakes are extended (about 1 second), and after about 4 seconds the aircraft approaches a 2-degree nose-down pitch and about 4 degrees left in roll. The transient response to speed brake retraction during a steady dive results in a nose-up pitching moment that improves the "pull-out" capability of the aircraft.

### Acceleration and Pitch

Accelerations from 100 knots with speed brakes retracted and extended were performed at constant altitude within 100 to 1500 feet. Entry speed was 100 knots, and exit speed was 150 knots. Figure 12 shows time histories of the deceleration with speed brakes retracted. Because of the constant altitude constraint, air longitudinal speed movement was gradual, resulting in a loss of wing lift as the aircraft pitched up. Roll is balanced by rolling to the left. Total time for the maneuver was 10 seconds. Figure 13 presents data with speed brakes extended. The roll rate is about 100 degrees per second for the roll. Loss of wing lift was about 1000 lbs. This was achieved with aft yoke, and the maneuver was completed with a roll rate of about 100 degrees per second. Total time for the maneuver was 10 seconds. Accelerations were also performed with speed brakes extended. The 10-degree turn, with all speed brakes, maintaining altitude at 1000 feet, was achieved with a roll rate of 100 degrees per second. Time to reach 100 degrees was 10 seconds, and exit speed was 150 knots. The maneuver was completed at a peak roll rate of 100 degrees per second. The roll rate was about 100 degrees per second. Mean roll rate for the 10-degree turn was 100 degrees per second.



One decelerating left turn was performed from 160 knots to 100 knots, using speed brakes. Deceleration time was 10.6 seconds, including a 1.2-second delay after brake extension before rolling into the turn. Brake retraction was initiated after passing 60-degree bank, which increased pitch rate and load factor. Thereafter, aft cyclic and down collective were employed to complete the maneuver. Mean turn radius was 530 feet. Main rotor pushrod loads were at approximately the same level as on previous turns, but stationary control loads were 50-60% higher.

#### COMPUTER SIMULATION STUDY

Appendix II describes the computer simulation and shows the comparison of simulation data with flight test data. The simulation was used to predict the effects on dive characteristics of increased brake effectiveness and stabilator bias angle, and to briefly study asymmetric brake deployment. The light aft load condition (2) was used, with a stabilator bias angle of 2.5 degrees.

#### Increased Brake Effectiveness

Figures 14 and 15, previously mentioned, show dive angle and fuselage angle of attack information developed at the 14,800-lb aft (#2) load condition with and without speed brakes. Figures 15 and 22 illustrate the effects of increased brake effectiveness. Additional brake area should be located on the lower ventral fin, where drag forces would align the airframe to the flight path and turbulence would not impinge on any control surfaces. The simulation results show that a dive angle of 30 degrees is possible at 160 knots. Also, the increased brake area further reduces variation in fuselage angle of attack.

#### Effect of Stabilator Bias Angle

The fuselage attitude,  $\alpha$ , was nose up relative to the flight path in a trimmed dive and varied with speed and rate of descent, reaching about 15 degrees at minimum torque. The speed brakes reduced angle of attack by up to 4 degrees (Figure 12) at a given dive angle and speed, but greater pitch control can be obtained by varying stabilator bias angle.

The dive characteristics were established using the simulator with a stabilator bias angle of 5 degrees leading edge up, relative to the neutral position, rather than the 1.5-degree flight test bias angle, to determine any significant change in angle of attack. From Figures 15 and 23, angle of attack is reduced by as much as 1 degree when stabilator bias is increased from 1.5 to 5 degrees.

### Asymmetric Deployment

A short study was conducted to predict the consequences of asymmetric speed brake deployment due to actuator malfunction. The simulator was used to determine controllability in high-speed level flight with every configuration of extended brake surfaces. Identification of the six brake surfaces is consistent with the original wind tunnel nomenclature Reference 1, and is shown in Figure 24.

Because of the asymmetry of lateral/directional control, the ability to trim the aircraft differs when considering left or right brake extensions. The simulations showed that when brakes are asymmetrically deployed, at forward speeds up to 180 knots, there is always sufficient roll control power to retrim the aircraft, although some deceleration will occur due to available power and/or collective limits. For example, if surfaces 1, 2, and 5 are opened at a forward speed of 180 knots, while 3, 4, and 6 remain closed, the aircraft will decelerate to about 160 knots because of the engine power limit, with the pilot able to restore and hold the aircraft at zero roll angle. At entry speeds below 145 knots, trim can be restored at the same speed following any configuration of speed brake deployment.

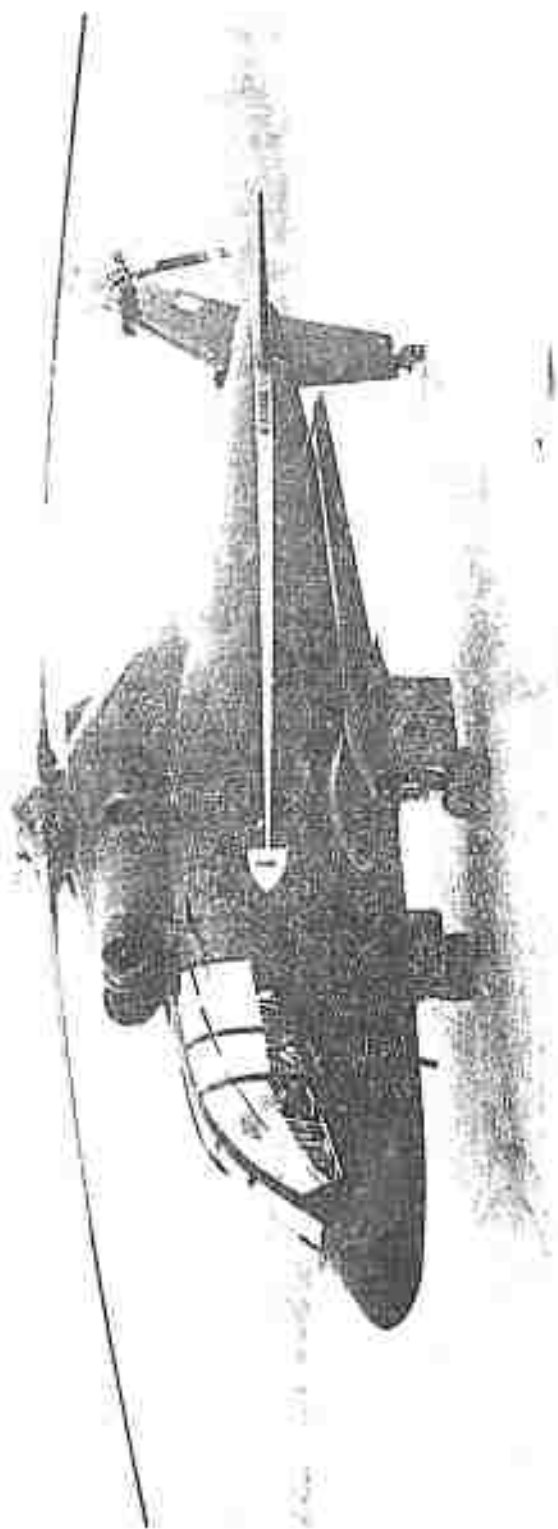
### CONCLUSIONS

The wing-mounted speed brakes on the S-67 aircraft increase dive angle and reduce the fuselage attitude relative to the flight path (fuselage angle of attack). They permit increases in dive angles from 5 to 7 degrees at 140 knots dependent upon the initial dive angle. At 160 knots, the increase in dive angle varies from 8 to 9 degrees. The increases in aircraft dive angle due to speed brake extension can be further increased if the aircraft is allowed to accelerate in the dive. For dive speeds greater than 120 knots, the fuselage angle of attack is reduced 4 to 5 degrees by extending the speed brakes. The increase in dive angle and/or the reduction in fuselage angle of attack while maintaining airspeed by the use of speed brakes improve the S-67 aircraft's capability as a weapons platform.

LITERATURE CITED

1. Gifford, J. A., ONE-TWELFTH SCALE WIND TUNNEL TESTS ON THE AH-3 (S-67) DEMONSTRATOR AIRCRAFT, SER-67000, Sikorsky Aircraft Division of United Aircraft Corporation, Stratford, Connecticut, April 1970.
2. Kaplita, T. T., S-67 STABILATOR INVESTIGATION, SER-67006, Sikorsky Aircraft Division of United Aircraft Corporation, Stratford, Connecticut, June 1971.
3. GENERAL REQUIREMENTS FOR HELICOPTER FLYING AND GROUND HANDLING QUALITIES, MIL-H-8501A, Amendment 1, April 1962.
4. Corso, J. J., and Kaplita, T. T., GENERAL HELICOPTER SIMULATION PROGRAM, SER 50542, Sikorsky Aircraft Division of United Aircraft Corporation, Stratford, Connecticut, May 1968.

Reproduced from  
best available copy.



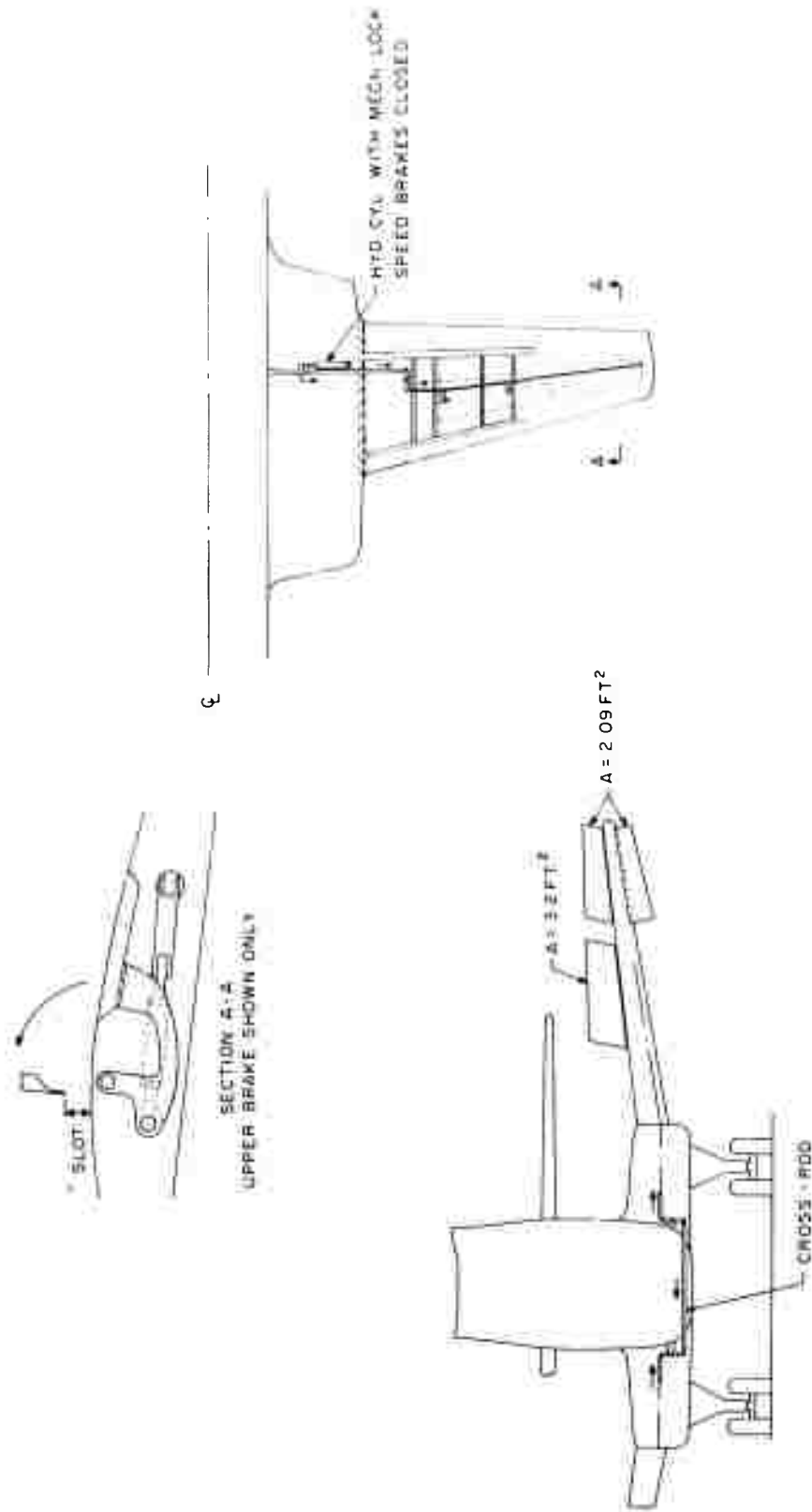


Figure 2. Speed Brake Areas and Locations.



Figure 3. In-Flight Front View, Speed Brakes Extended.

Reproduced from  
best available copy.



Figure 4. In-Flight Front View, Speed Brakes Extended.

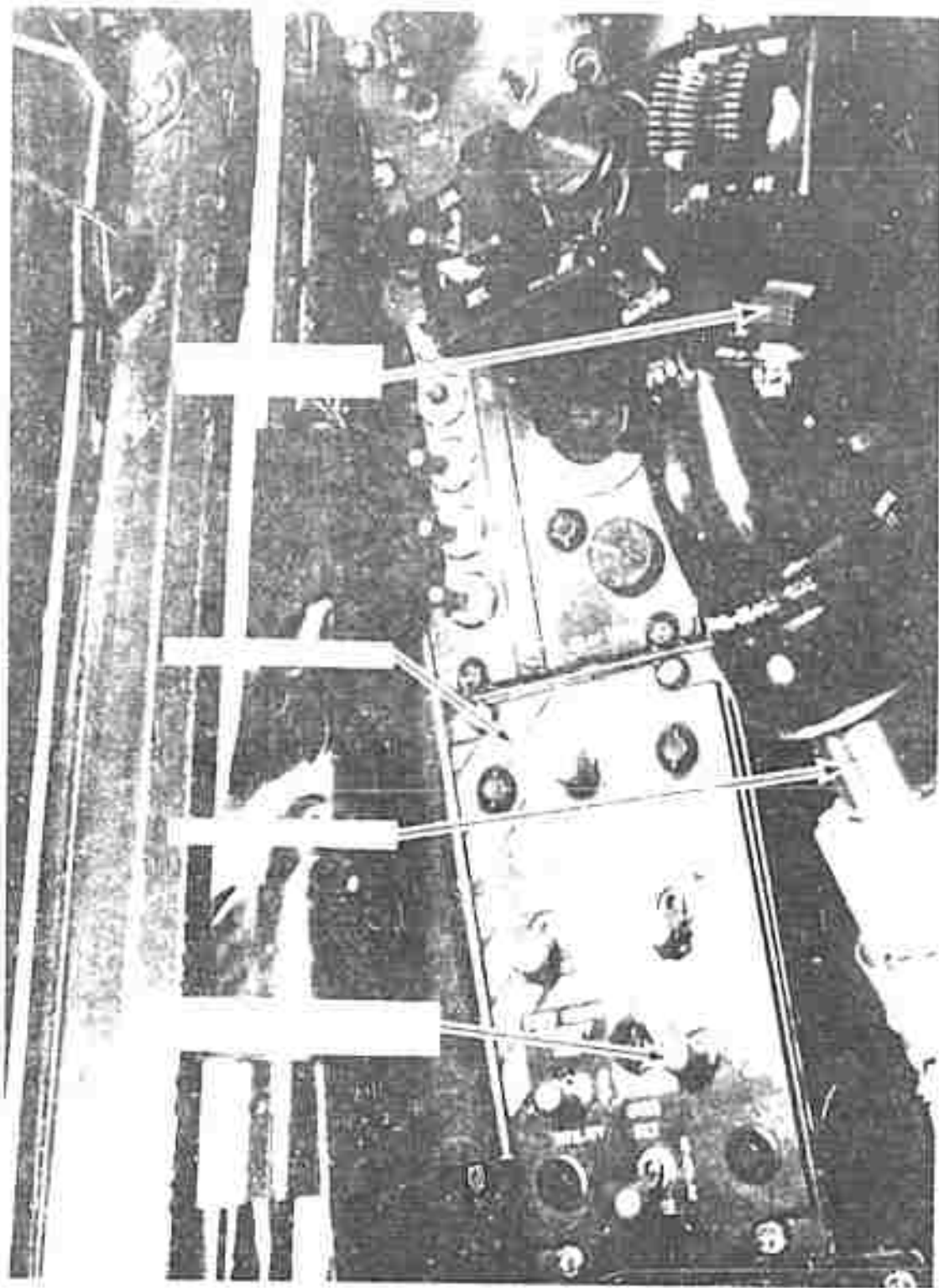






Fig. 1.  $\log_{10} R$  vs  $\log_{10} t$ .  
 $\log_{10} R = \log_{10} t$

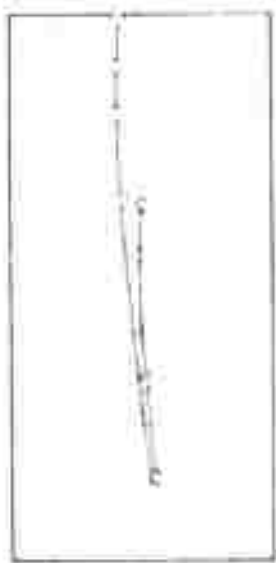


Fig. 2.  $\log_{10} R$  vs  $\log_{10} t$ .  
 $\log_{10} R = \log_{10} t$



Fig. 3.  $\log_{10} R$  vs  $\log_{10} t$ .  
 $\log_{10} R = \log_{10} t$



Fig. 4.  $\log_{10} R$  vs  $\log_{10} t$ .  
 $\log_{10} R = \log_{10} t$

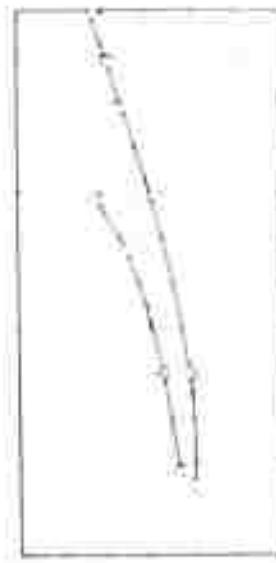


Fig. 5.  $\log_{10} R$  vs  $\log_{10} t$ .  
 $\log_{10} R = \log_{10} t$



Fig. 6.  $\log_{10} R$  vs  $\log_{10} t$ .  
 $\log_{10} R = \log_{10} t$

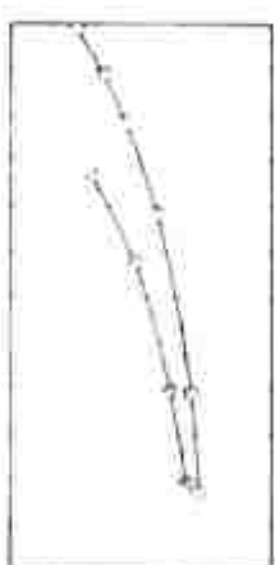
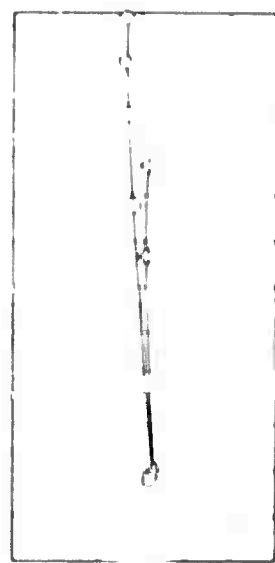
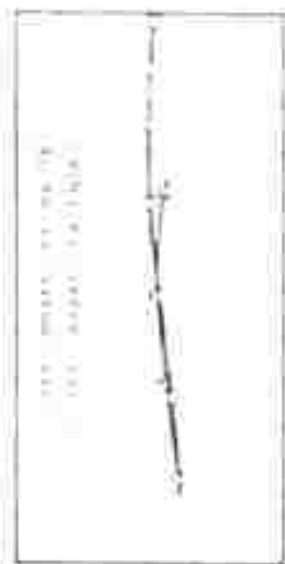
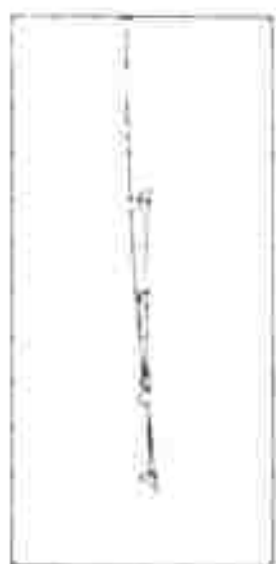


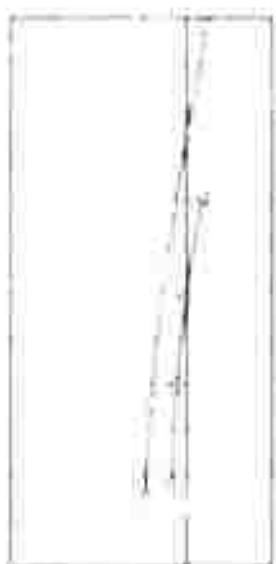
Figure 1. Stick Position vs. Forward Speed. Data collected from the flight test.



Graph 1: Y vs X



Graph 2: Y vs X



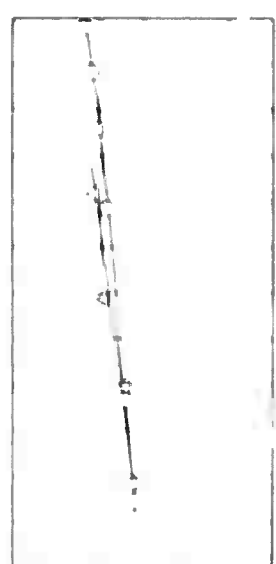
Graph 3: Y vs X



Graph 4: Y vs X



Graph 5: Y vs X



Graph 6: Y vs X

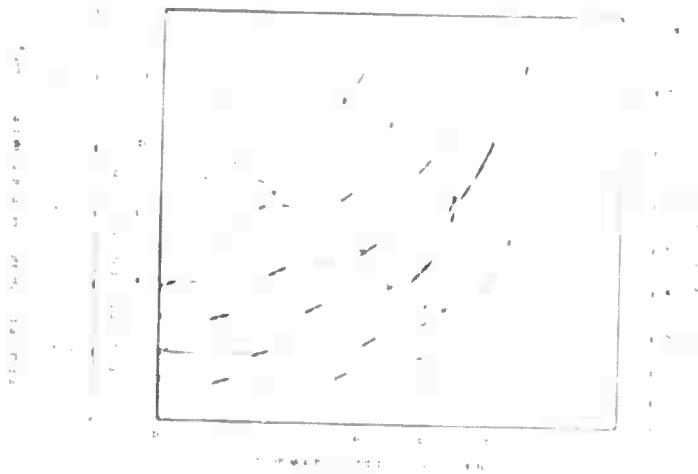


Figure 1. Relationship between  $A_{100}$  and  $A_{1000}$  for various values of  $A_{1000}$ .

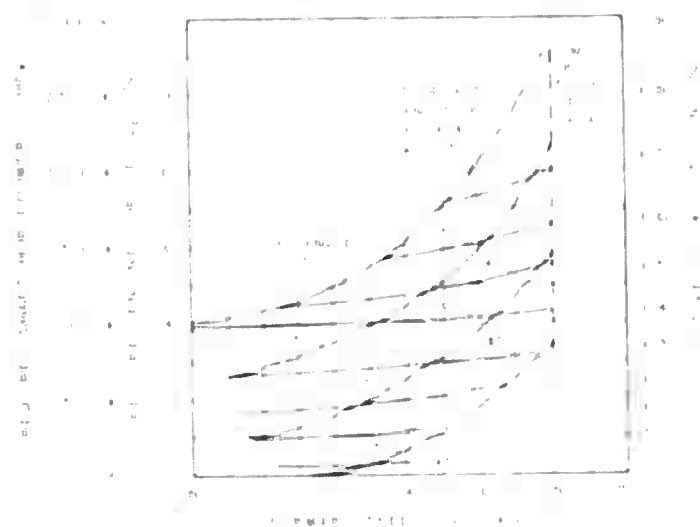


FIGURE 1. (a) and (b)

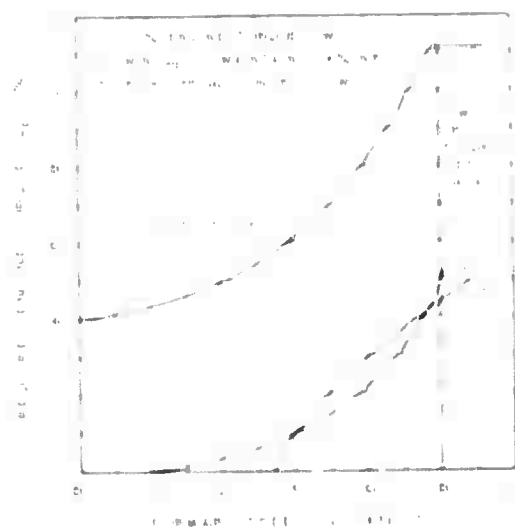


FIGURE 2. (a) and (b)

Figure 1. (a) and (b) are data points, (c) and (d) are theoretical curves.

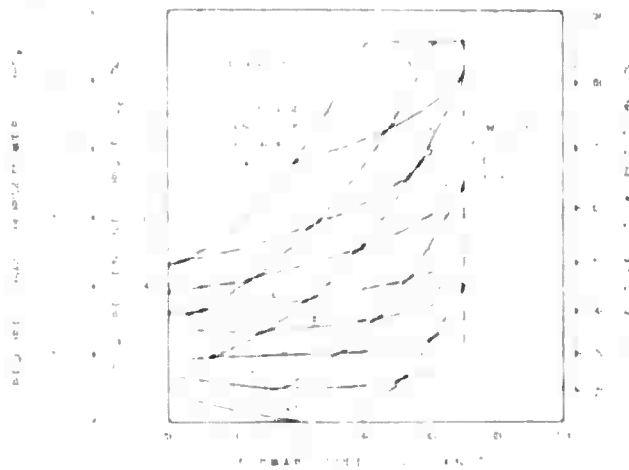
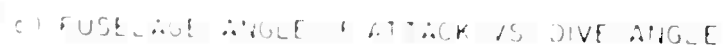
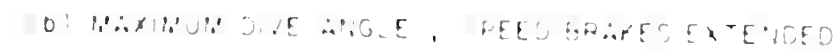


FIGURE 10. STRESS VERSUS STRAIN.



FIGURE 11. STRESS VERSUS STRAIN.

Figure 10. Stress Characterization,  $W = 11,300$  lb.,  
of 70-30 Brass Extended.



16

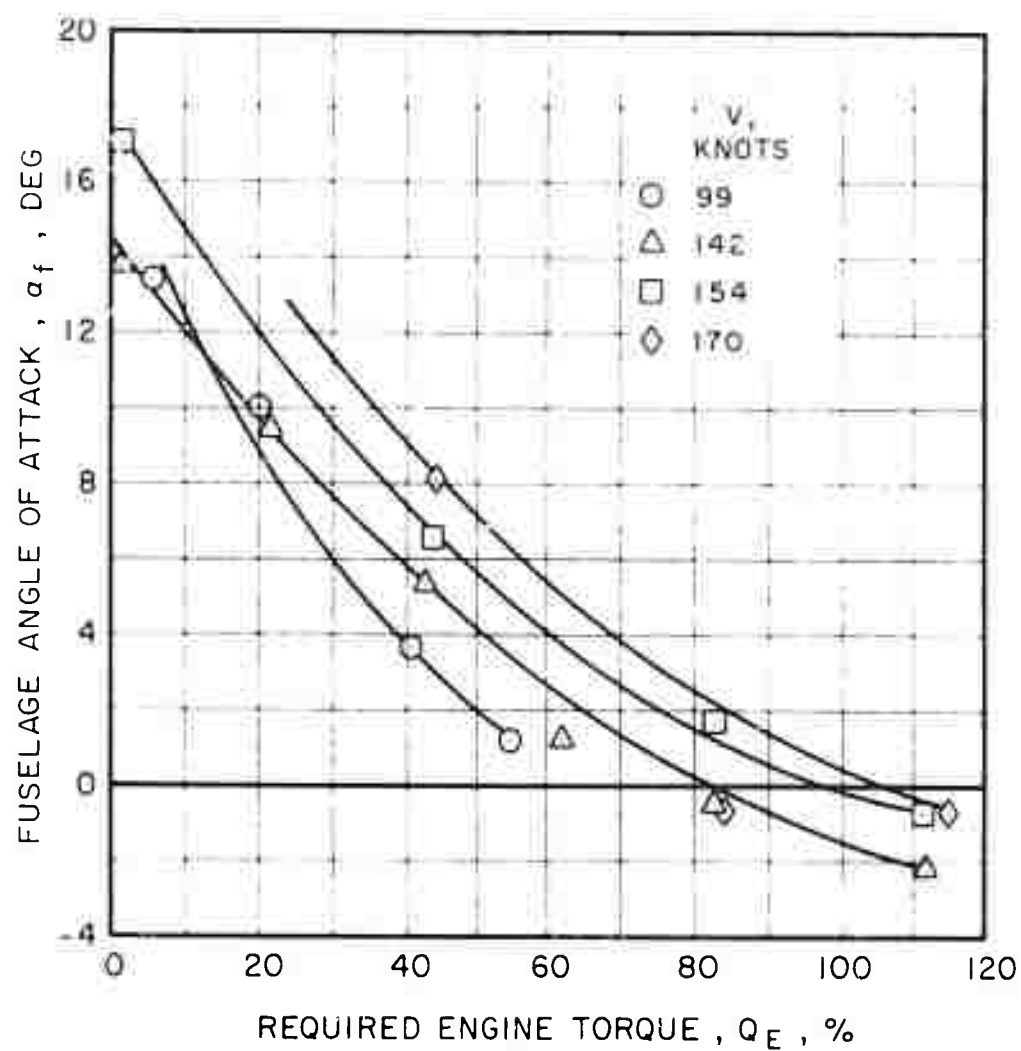


Figure 13. Fuselage Angle of Attack vs. Engine Torque and Forward Speed,  $W = 17,000$  lb,  $cg = 170$  in., Speed Brakes Extended.



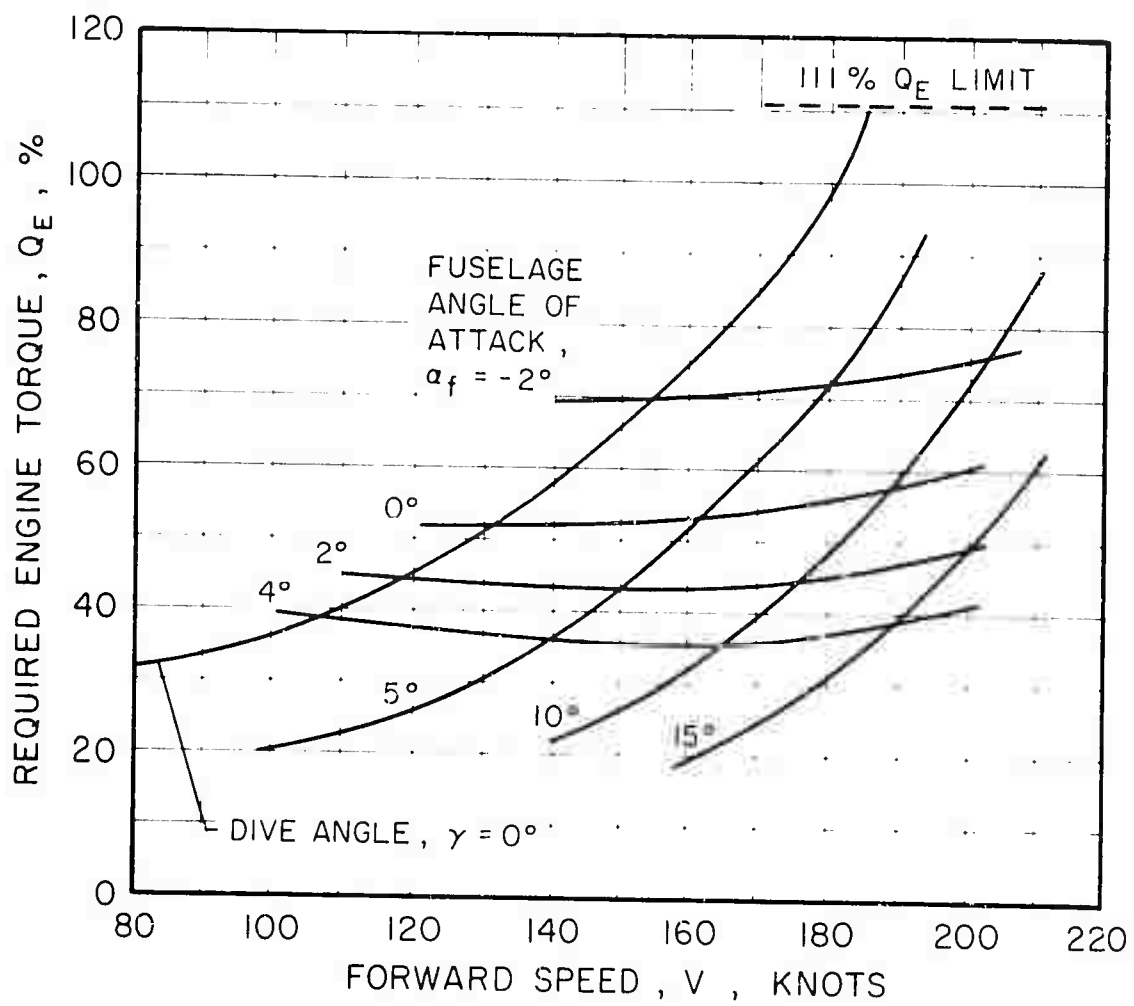


Figure 14. Simulation of Dive Characteristics, Speed Brakes Retracted, GW = 14,800 lb, cg = 276 in.

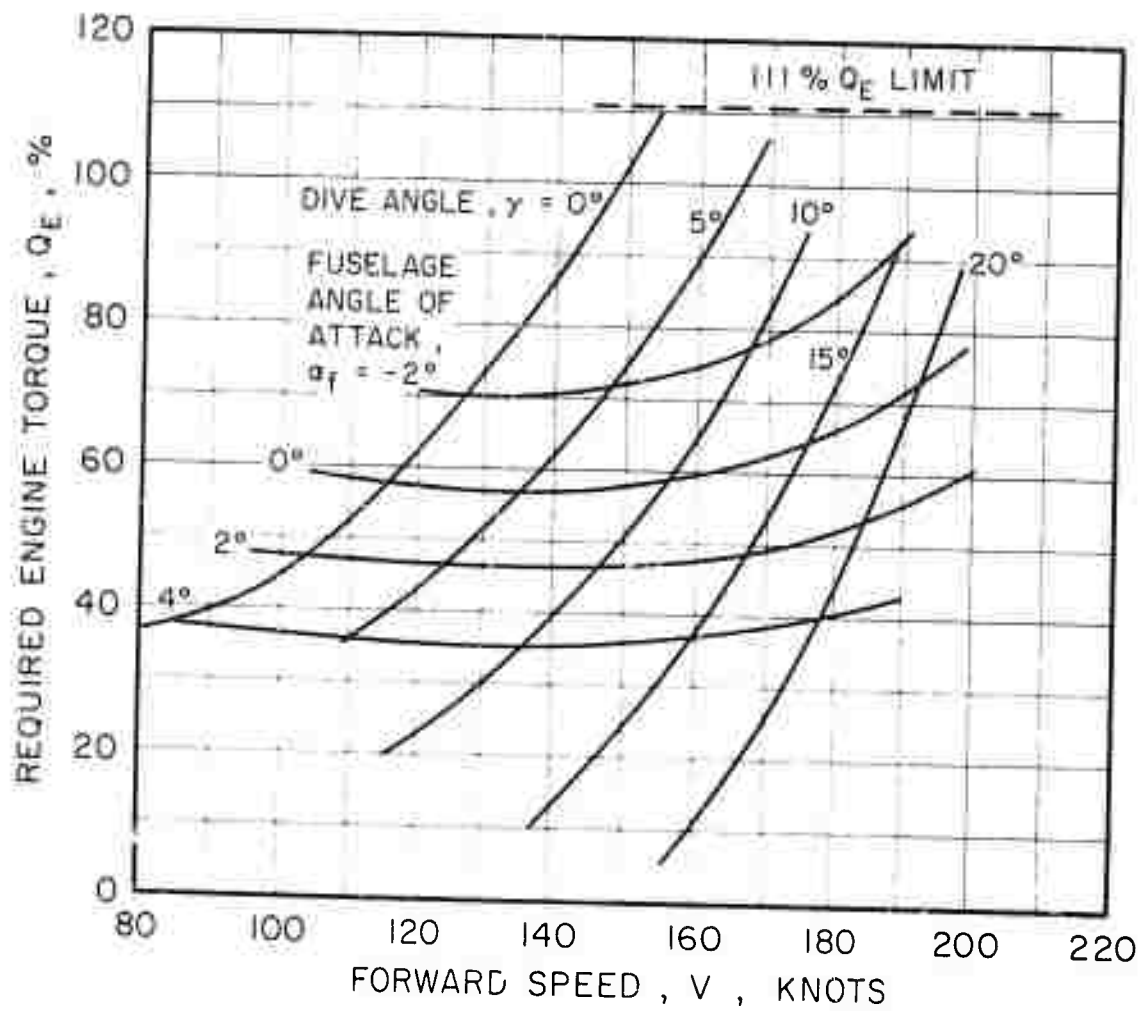


Figure 15. Simulation of Dive Characteristics, Speed Brakes Extended,  $GW = 14,800$  lb,  $cg = 276$  in.

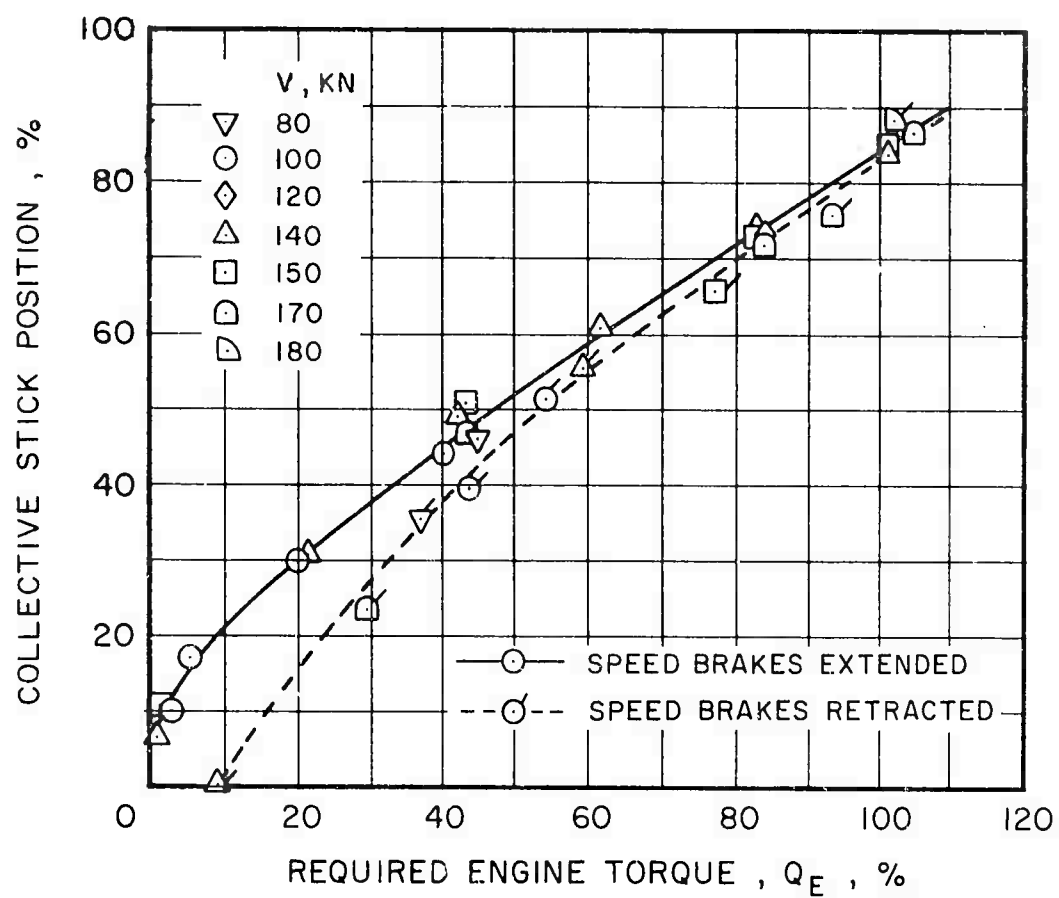


Figure 16. Collective vs. Engine Torque,  $GW = 17,300$  lb,  $cg = 276$  in.

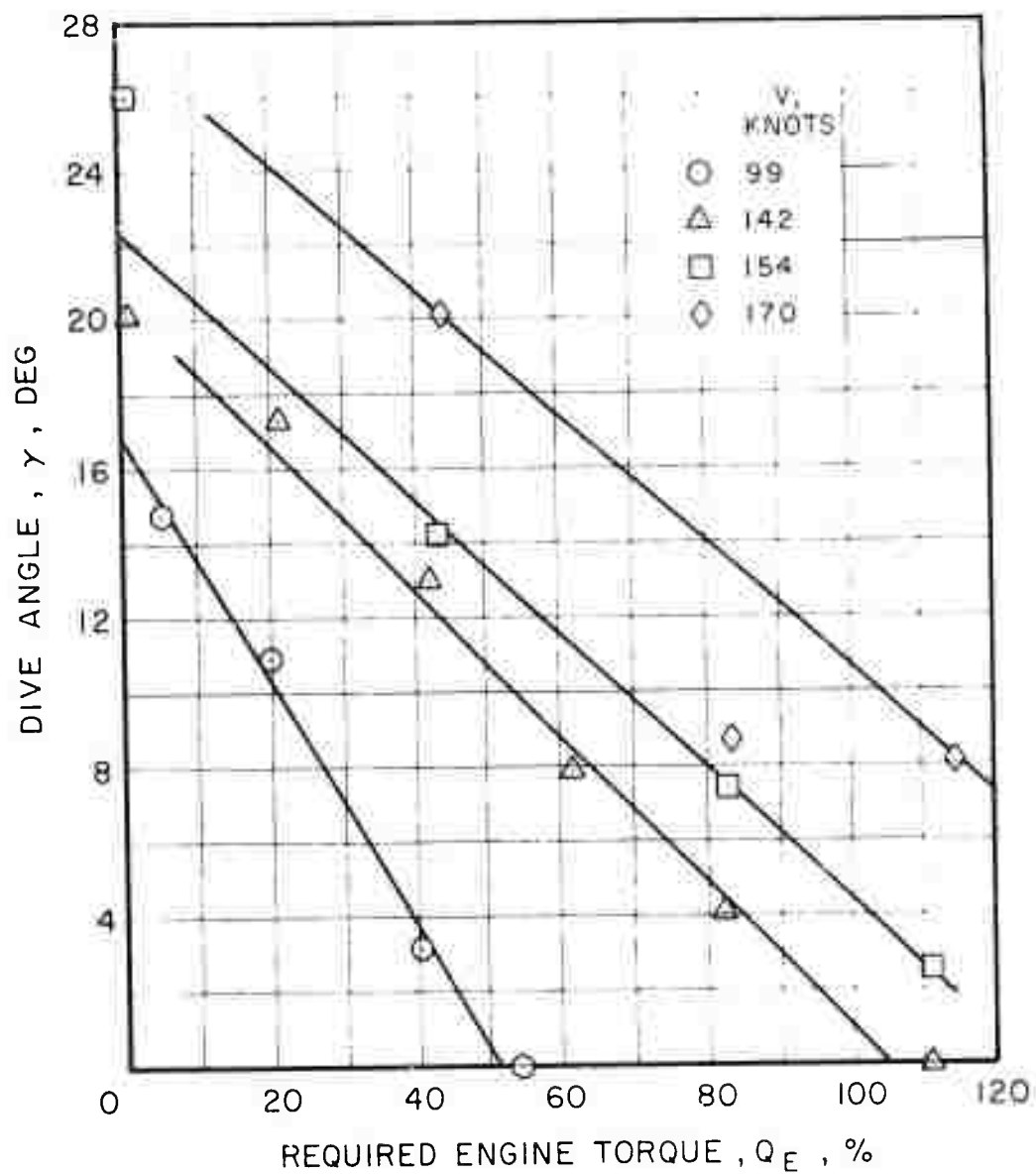


Figure 17. Dive Angle vs. Engine Torque and forward speed.  
 GW = 17,300 lb, cg = 276 in., Speed brake extended.

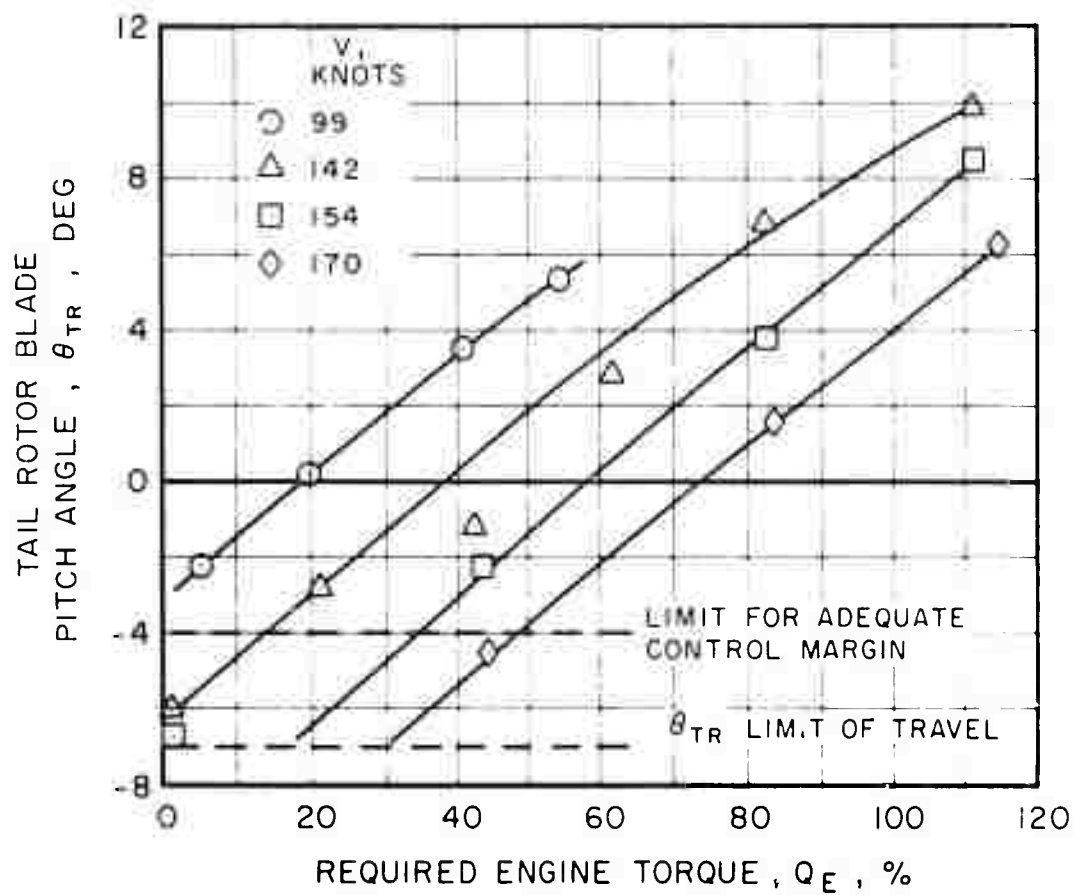


Figure 18. Tail Rotor Pitch vs. Engine Torque and Forward Speed,  $W = 17,400$  lb,  $cs = 70$  in., Speed Brakes extended.

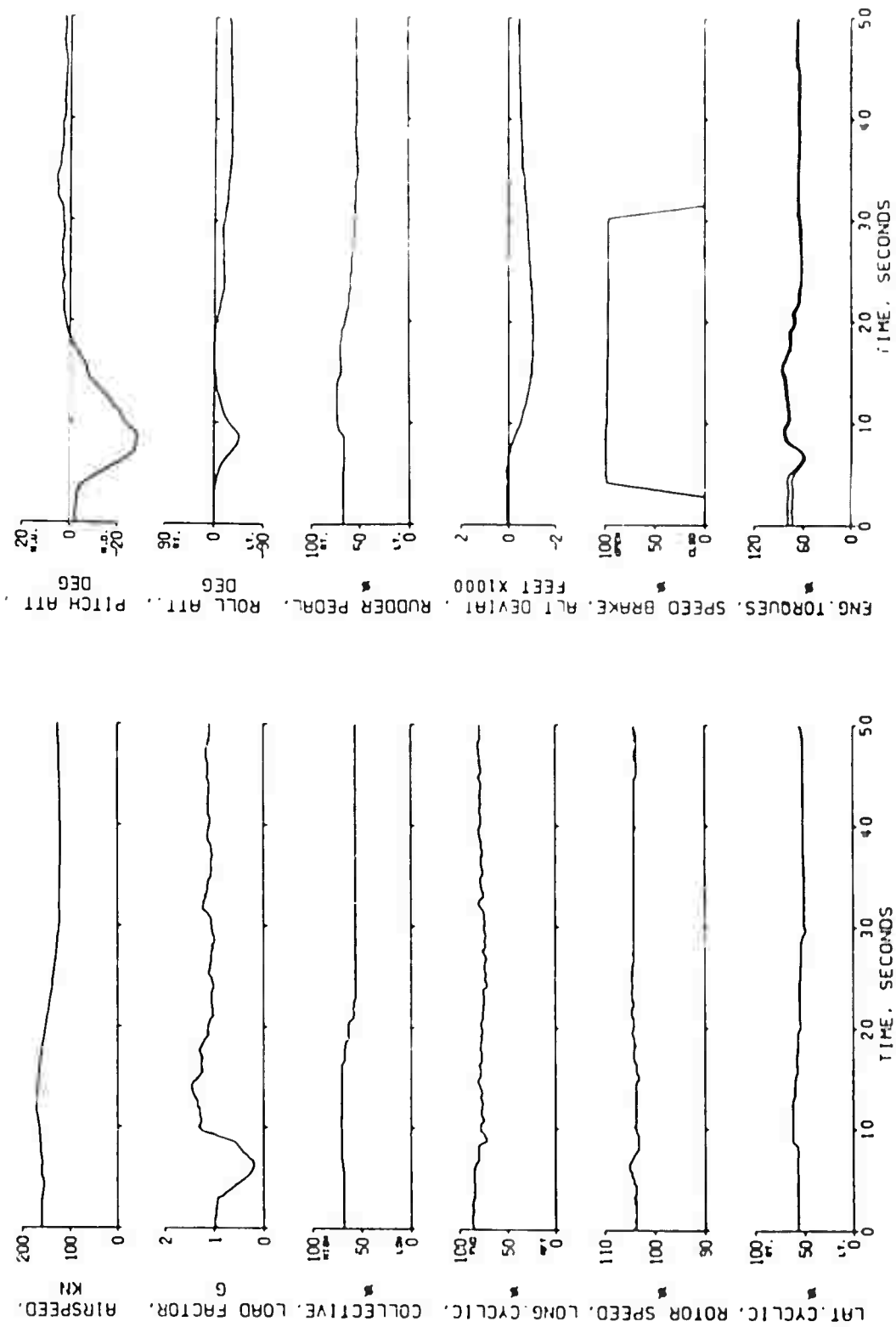
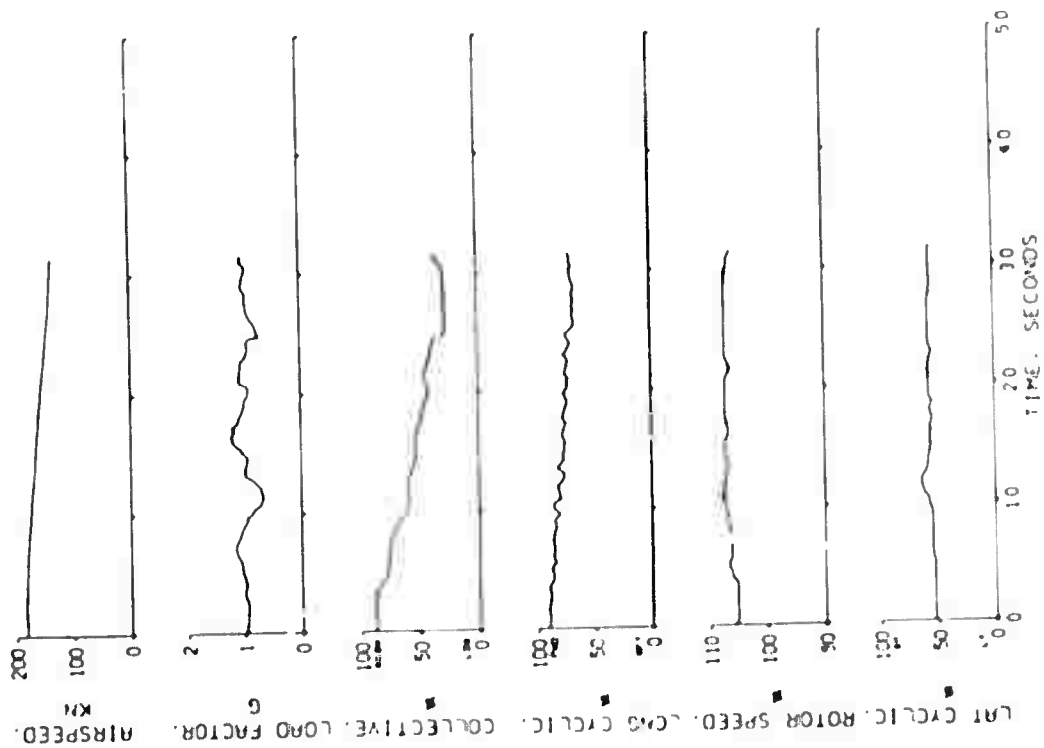
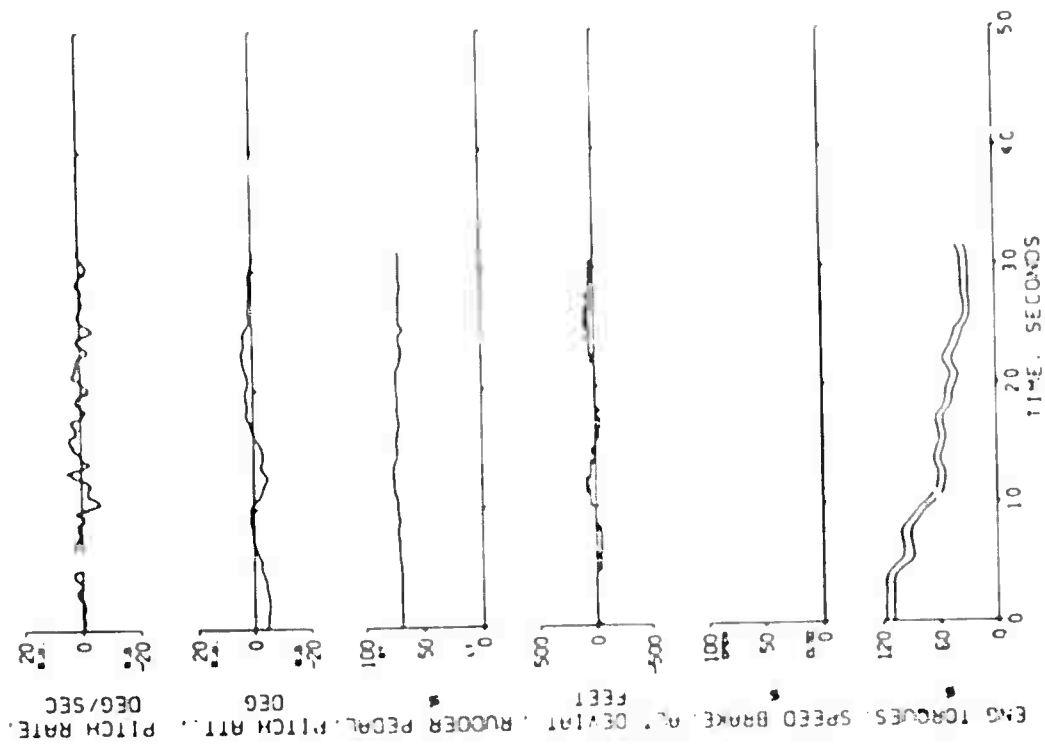
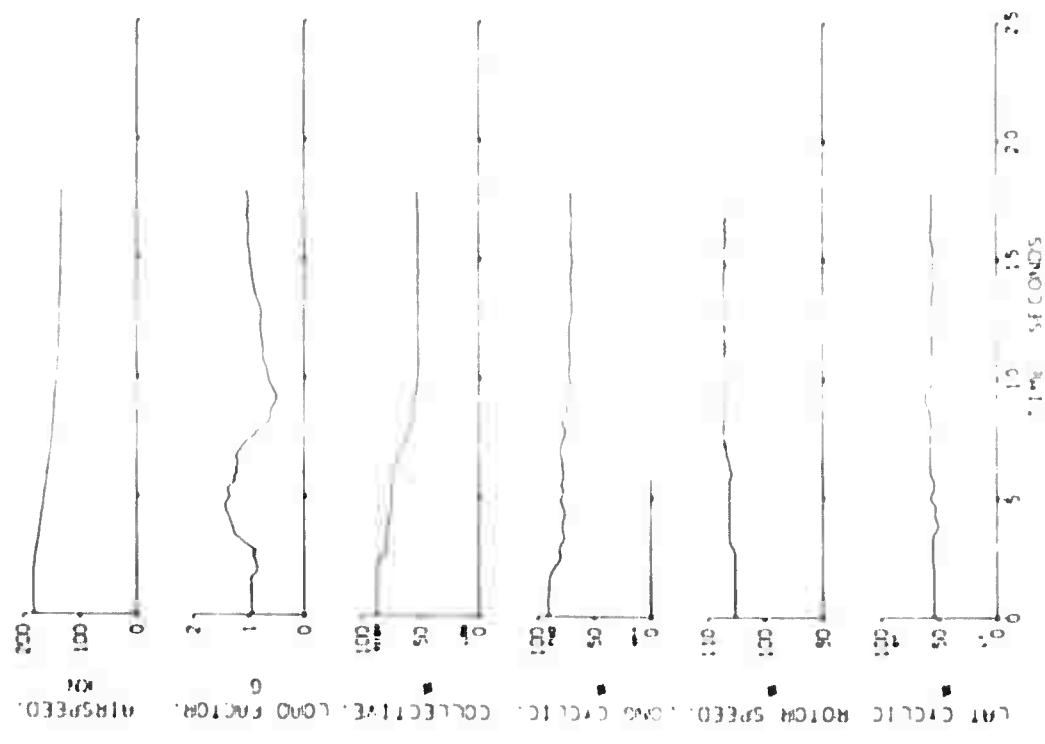
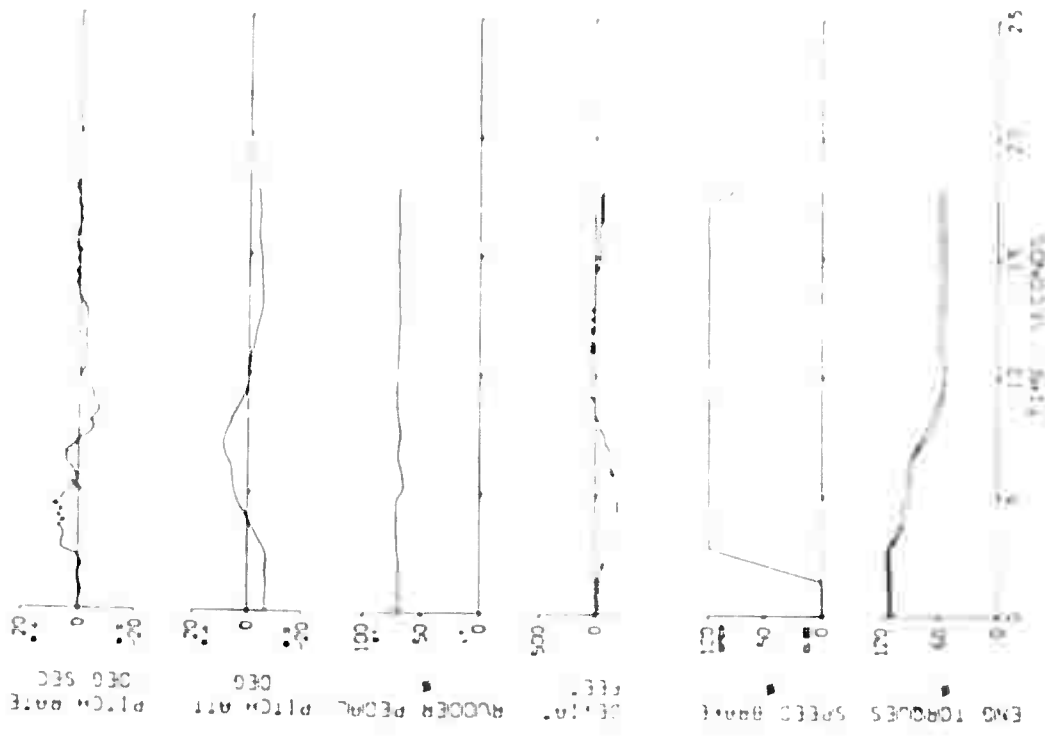


Figure 19. Transient Effects of Speed Brake Extension at  
V = 180 kt, Controls Fixed.









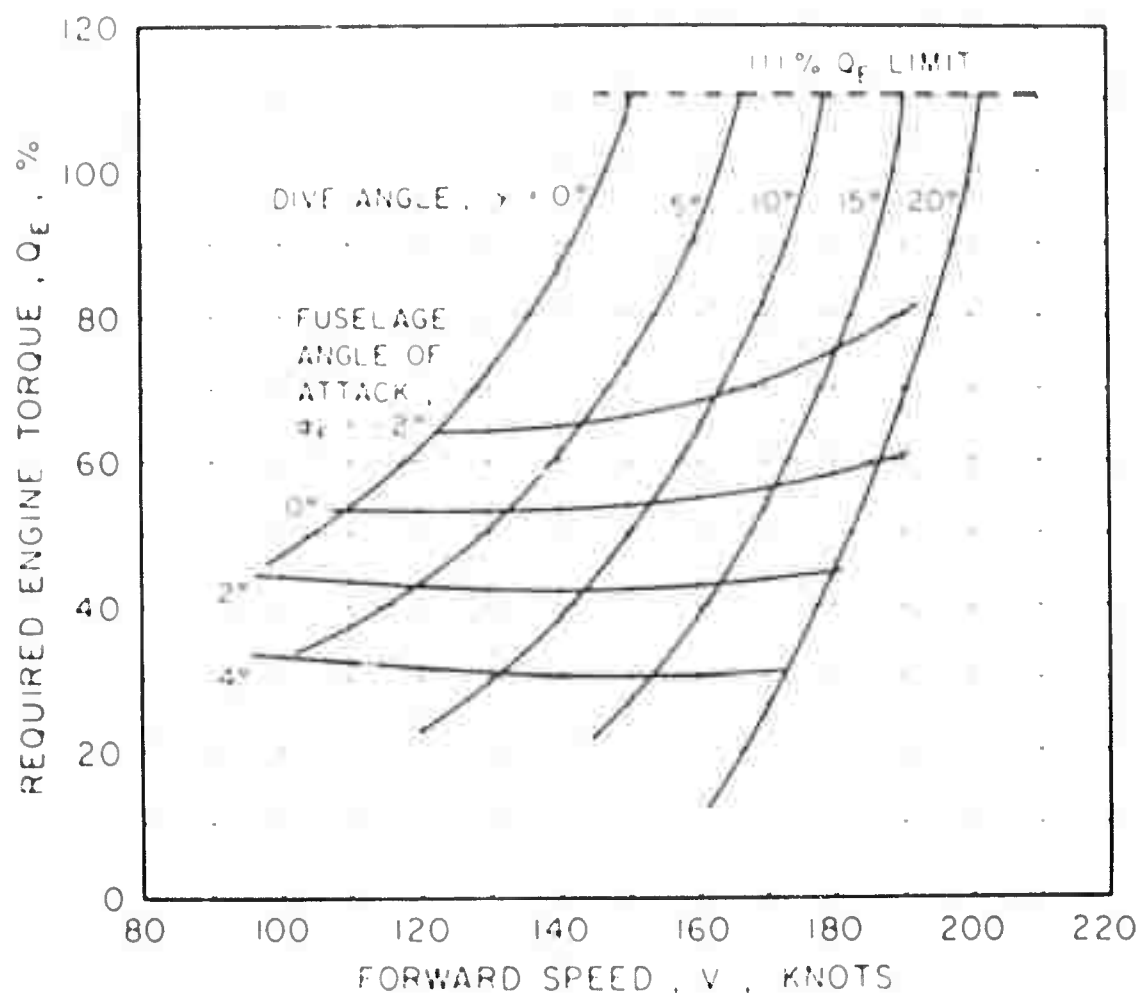
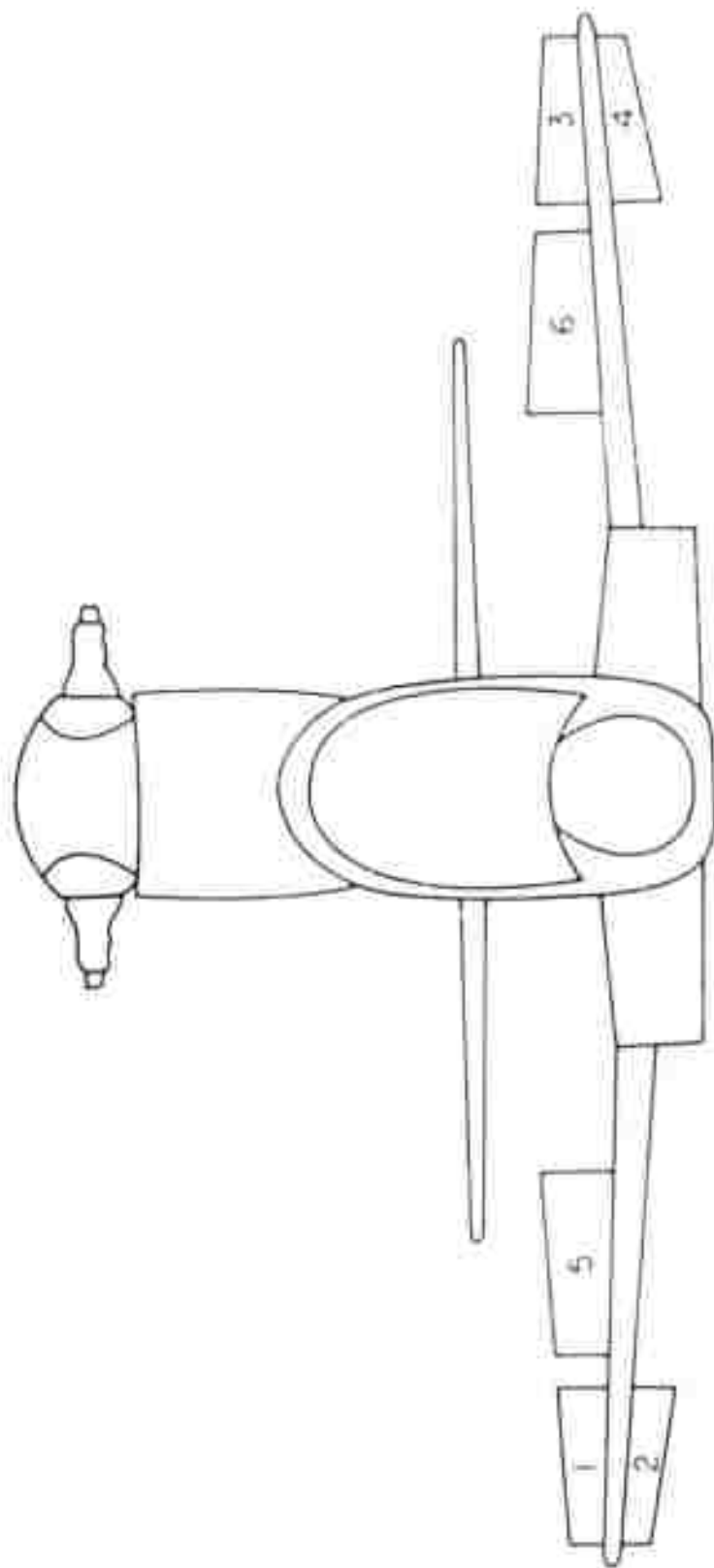


Figure 1. Required engine torque,  $Q_E$ , % vs forward speed,  $V$ , knots for various dive angles,  $\gamma$ , and fuselage angles of attack,  $\alpha$ . The curves are for a standard aircraft configuration.



— 1 —

2.

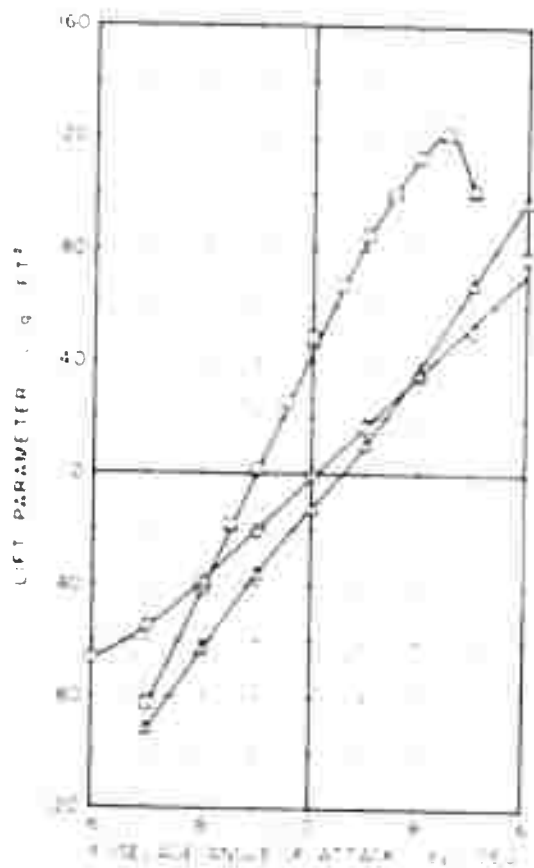


Figure 1.5. C-47 Wind Tunnel Data, Showing Lift, Pitching Moment, and Drag vs. Fuselage Angle of Attack for Total Aircraft Less Wings, With Wings, and Speed Brakes Retracted and Extended.

## APPENDIX II

### COMPUTER SIMULATION STUDY

#### DESCRIPTION

The General Helicopter Simulation Program described in Reference 4 was adapted to Sikorsky Aircraft's PDP-10 digital computer to simulate the S-67. The six-degree-of-freedom simulation used a rotor model with a rigid five-bladed four-segmented blade element analysis including the rotor flapping degree of freedom. Nonlinear steady-state rotor blade airfoil section aerodynamic data were used that include the effects of stall and compressibility. Two-dimensional flow was assumed at each section of the blade.

Wind tunnel data from a one-twelfth scale model test of the S-67, Reference 1, were used to describe the force and moment contributions of the combined wing, fuselage, stabilator, and vertical tail. Speed brake contributions to the aircraft forces and moments were incorporated as additional components to those for the basic aircraft. The wind tunnel data included the effects of aircraft angle of attack and stabilator incidence on lift, drag, and pitching moment.

#### CORRELATION WITH FLIGHT TEST DATA

##### Hover

In hover, two adjustments to the simulation were necessary to obtain satisfactory correlation. Main rotor blade twist was increased by 2 degrees, and a 2-inch lateral center-of-gravity shift to the left was applied at the light gross weight conditions.

The S-67 rotor blades show some degree of aerodynamic twisting with the 20-degree swept tips. Under normal trimmed flight conditions, the blade loadings are high at the blade tip. Since the center of pressure of the swept tip is behind the blade torsional axis, aeroelastic twisting results.

The lateral center-of-gravity offset to the left brought the trim lateral cyclic requirement into agreement with flight test data. This center-of-gravity offset is expected, since the tail rotor and the vertical tail are positioned to the left of the aircraft centerline.

##### Forward Flight

In forward flight, the blade aerodynamic twist correction for collective pitch correlation varied with speeds above 80 knots. Above this speed the correction diminished linearly to -0.5 degree at 182 knots. A leading-edge-up stabilator bias angle correction of 2 degrees was needed to correlate longitudinal cyclic and aircraft attitude. This is due to some inaccuracies in predicting main rotor downwash at the stabilator.

Figure 26 shows the results of the correlation in hover and forward flight for the light-gross-weight aft-center-of-gravity condition, with speed brakes retracted and zero stabilator bias angle. Specific flight test points were simulated using the proper gross weight and density altitude. From hover to 80 knots, the simulation points are connected by a dotted line to indicate that no correlation was attempted in the low-speed regime.

At high speed, the rotor model requires extremely high power at moderate rotor stall. This is because two-dimensional flow at the rotor blade section was used, omitting the spanwise component.

To correlate flight test values of longitudinal cyclic and aircraft pitch attitude in forward flight with speed brakes extended, a reduction in the pitching moment was necessary, equivalent to that produced by 9 square feet of drag area. The wind tunnel model speed brakes were fixed flush to a solid wing, whereas the extended brakes on the S-67 leave a hole through the wing and a 1-inch slot between the brake panel and the wing, as shown in Figure 2. The resulting aerodynamic inconsistencies between wind tunnel and flight test conditions, and the shortcomings of the rotor model mentioned above, hindered exact simultaneous correlation of aircraft attitudes, control quantities and rotor power in level flight.

Figures 27 through 29 show the results of the correlation for different gross weights, center-of-gravity positions, and stabilator biases.

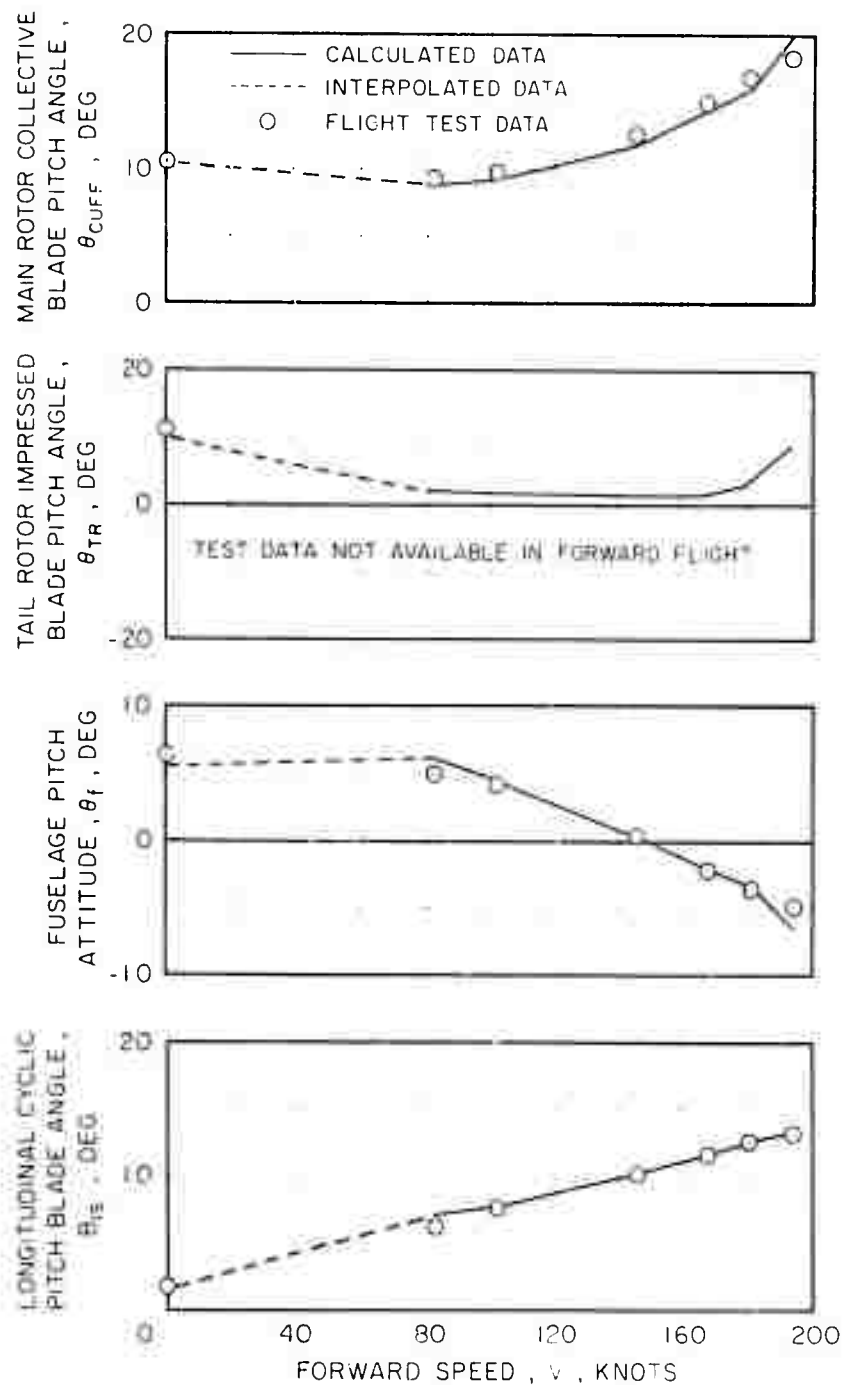


Figure 26. Comparison Between Simulated and Flight Test Data, Level Flight Trim,  $GW = 14,000$  lb,  $cg = 1.76$  in., Stabilator Bias = 0 deg, Speed brakes Retracted.



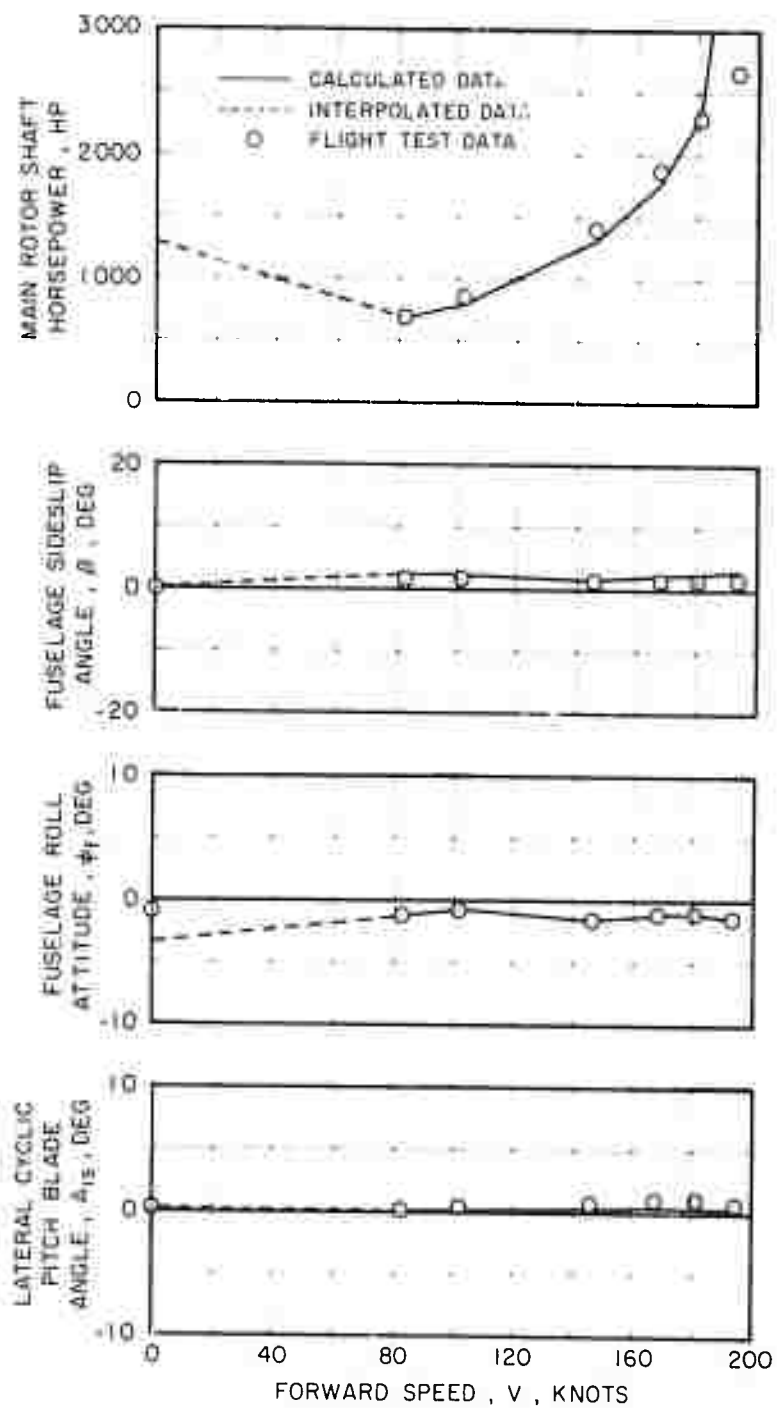


Figure 26. Concluded.

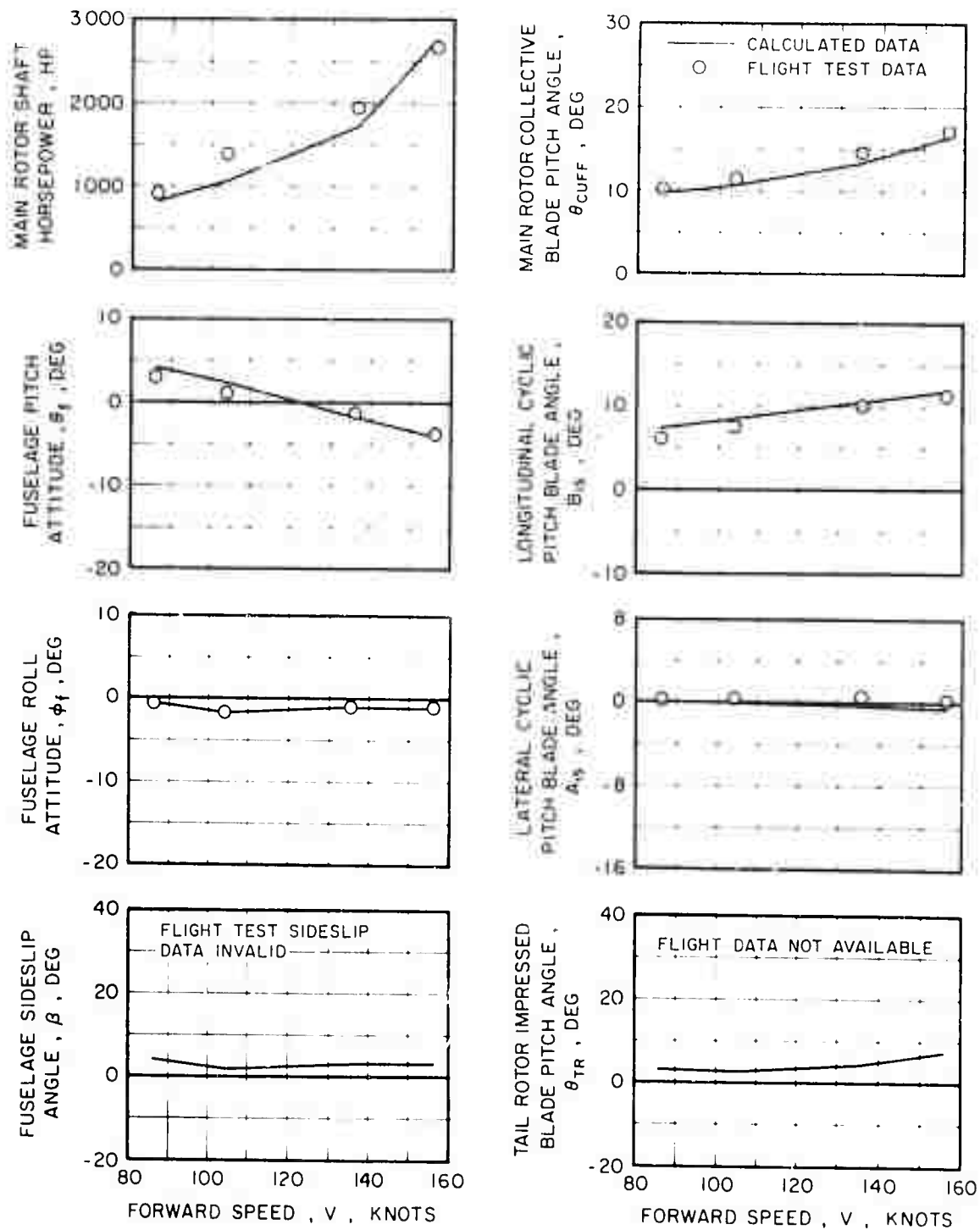


Figure 27. Comparison Between Simulated and Flight Test Data, Level Flight Trim, GW = 14,500 lb, cg = 275 in., Stabilator Bias = 0 deg, Speed Brakes Extended.

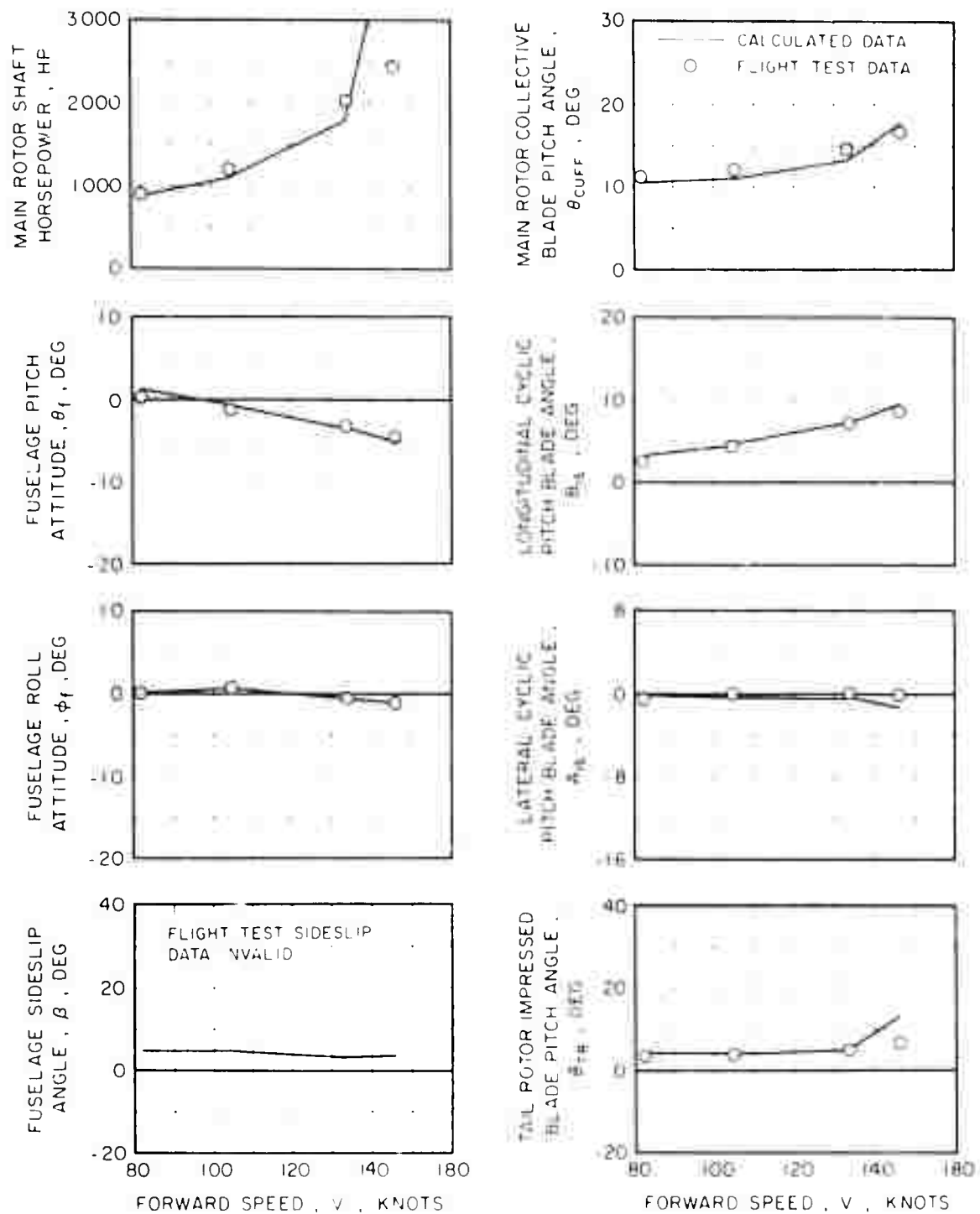


Figure 28. Comparison between Calculated and Flight Test Data, Level Flight Trim,  $W = 10,000$  lb,  $W_F = 1.25$  lb, Stabilizer Pitch = 0 deg, Speed Brakes Extended.

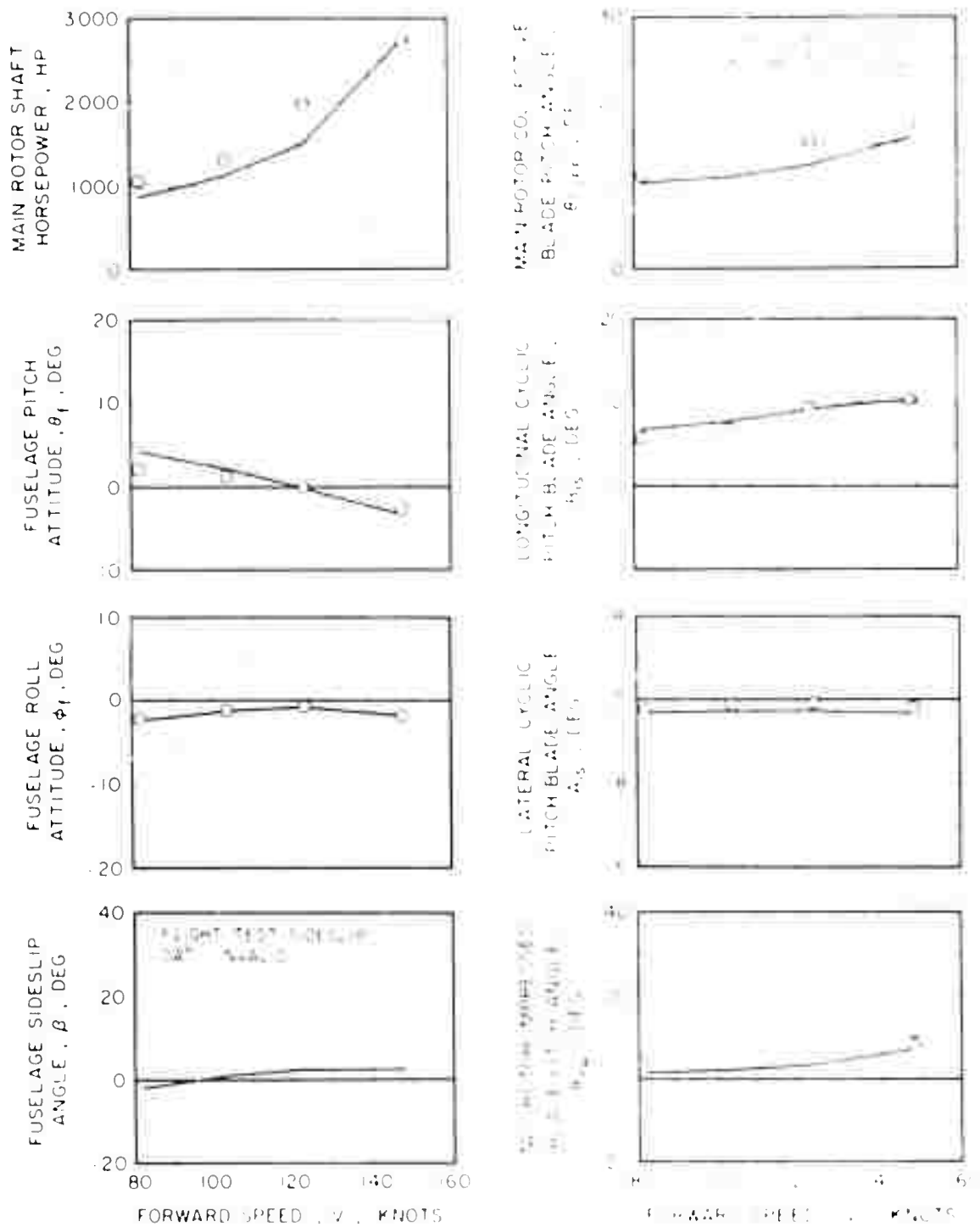


FIGURE 29. Performance characteristics of the Sikorsky HO4S helicopter. Data were obtained from the flight test program conducted at the Sikorsky Aircraft Company, Stratford, Connecticut, in 1961.